Investigation of Fatigue Crack Growth Rates Under Variable Amplitude Loading

by

Asim Rauf

A Thesis Presented to the

FACULTY OF THE COLLEGE OF GRADUATE STUDIES

KING FAHD UNIVERSITY OF PETROLEUM & MINERALS

DHAHRAN, SAUDI ARABIA

In Partial Fulfillment of the
Requirements for the Degree of

MASTER OF SCIENCE

In

MECHANICAL ENGINEERING

June, 1995

Investigation of Fatigue Crack Growth Rates Under Variable Amplitude Loading

BY

Asim Rauf

A Thesis Presented to the

FACULTY OF THE COLLEGE OF GRADUATE STUDIES

KING FAHD UNIVERSITY OF PETROLEUM & MINERALS

DHAHRAN, SAUDI ARABIA

In Partial Fulfillment of the
Requirements for the Degree of

MASTER OF SCIENCE
In
MECHANICAL ENGINEERING

June, 1995

KING FAHD UNIVERSITY OF PETROLEUM AND MINERALS
DHAHRAN, SAUDI ARABIA
COLLEGE OF GRADUATE STUDIES

This thesis, written by

Asim Rauf

under the direction of his Thesis Advisor, and approved by his Thesis committee, has been presented to and accepted by the Dean, College of Graduate Studies, in partial fulfillment of the requirements for the degree of

MASTER OF SCIENCE IN MECHANICAL ENGINEERING

Thesis Committee :

Dr. Zafarullah Khan (Chairman)

Dr. Anwar K. Sheikh (Co-Chairman)

Dr. Ibrahim M. Allam (Member)

Dr. Furrukh S. Qureshi (Member)

Department Chairman (Mech. Engg.)

Dean, College of Graduate Studies

Date: 22-7-95

Dedicated to

my beloved parents

whose prayers, inspiration and love led to this accomplishment

Acknowledgment

In the name of Allah, Most Gracious, Most Merciful. Read in the name of thy Lord and Cherisher, Who Created man from a {leech-like } *clot. Read and thy Lord is Most Bountiful. He Who taught* {*the use of*} *the pen. Taught man that which he knew not. Nay, but man doth transgress all bounds. In that he looketh upon himself as self-sufficient. Verily, to thy Lord is the return* {*of all*}.

(The Holy Quran, Surah Al-A'alaq, No.96)

First and foremost, all praise to Allah, *subhanahu-wa-ta'ala*, the Almighty, Who gave me an opportunity, courage and patience to carry out this work. I seek His mercy, favor, and forgiveness. I feel priviledged to glorify His name in the sincerest way through this small accomplishment. May He, *subhanahu-wa-ta-Aaala*, guide me and the whole humanity to the right path *(Aameen)*.

Acknowledgement is due to King Fahd University of Petroleum & Minerals for providing support to this research work.

I am indebted to my thesis advisor, Dr. Zafarullah Khan for his help and advice. I acknowledge him for his valuable time, encouragement and guidance during various stages of this work.

I am grateful to my thesis co-advisor, Dr. Anwar K. Sheikh and committee member Dr. Ibrahim M. Allam for their interest, constructive criticism and understanding. Thanks are also due to the my thesis committee member, Dr. Furrukh S. Qureshi for his comments and critical review of the thesis.

I am thankful to the department chairman, Dr. M. Budair and other faculty members especially Mr. Younas and Mr. Aleem for their help and cooperation.

Notable mentions go to all my friends on the campus especially Zaka, Ikram, Amir, Nayyar, Salman and Asif who provided a wonderful company and support.

Last but not the least, thanks are due to the members of my family for their emotional and moral support throughout my academic career. No personal development could ever take place without the proper guidance of parents. This work is dedicated to my parents for taking pains to fulfill my personal and academic pursuits and shaping my personality. I am also grateful to both of my brothers, Amir and Adil, for their support, motivation, constant inspiration and encouragement. I also acknowledge with gratitude, the affection and love of my sisters.

Contents

List of Tables

List of Figures

Nomenclature

a	crack length
a_f	final crack length
a_i	initial crack length
a_o	crack length before the overload
a_p	sum of crack length before the OL and the OL plastic zone size
C	Paris constant (the y-intercept on crack growth curve)
C_p	Wheeler's retardation coefficient
$\frac{da}{dN}$	fatigue crack growth rate
$f(g)$	the geometric factor
K_c	fracture toughness
K_{max}	maximum stress intensity
K_{OL}	stress intensity factor at the overload
ΔK	stress intensity factor range
ΔK_{eff}	effective stress intensity factor
m	Paris co-efficient (slope of crack growth curve)
n	number of cycles in the base constant amplitude cycle
N	total number of life cycles
N_p	number of crack propagation life cycles
p	Wheeler's shaping exponent

P	applied load
ΔP	range of applied load
P_{max}	maximum load applied in the cycle
P_{mean}	mean load of cycle
P_{min}	minimum load applied in the cycle
r_y	plastic zone size
r_{OL}	overload plastic zone size
R	stress ratio
ρ	radius of the notch
σ	nominal stress at crack tip
σ_{alt}	mean stress at the crack tip
σ_{max}	maximum stress at crack tip
σ_{mean}	mean stress at crack tip
σ_{min}	minimum stress at crack tip
σ_{OP}	crack opening stress
$\sigma_{Y.S}$	tensile yield strength of the material
t	thickness of the specimen
U	effective stress parameter
w	width of the specimen

Abstract

Name: Asim Rauf

Title: Investigation of Fatigue Crack Growth Rates Under Variable Amplitude Loading

Major Field: Mechanical Engineering

Date of Degree: June, 1995

The study of fatigue crack growth rate is an important consideration in design of engineering components and during their service life. The basic problem of load interaction (overload excursions) under variable amplitude loading is addressed in this thesis. An experimental program is designed to collect the actual fatigue life data under differnt VAL conditions. Two fatigue crack propagation life prediction models, namely the Wheeler model (using Paris and modified Paris equations) and Elber's model have been employed to predict the fatigue crack propagation life analytically. The results of these analytical fatigue life predictions show good agreement with the experimental fatigue life data.

Fractographic study is also conducted to obtain microscopic fatigue crack growth rates based on the study of fatigue striations using scanning electron microscope (SEM). The fractographic result have been used succesfully to correlated the observed macroscopic crack growth rates with the microscopic crack growth rates with reasonably good accuracy.

Master of Science Degree
Department of Mechanical Engineering
King Fahd University of Petroleum and Minerals
Dhahran, Saudi Arabia
June, 1995

ملخص

الإسم : عاصم رؤوف

الموضوع : بحث تطور نمو الشرخ الكلالي تحت تأثير أحمال مختلفة متكررة الإتساع ٠

التخصص : هندسة ميكانيكية

التاريخ : يونيو ١٩٩٥

إن دراسة معدل نمو وتطور الشرخ الكلالي تعتبر مهمة جدا عند تصميم الأجزاء الهندسية وخلال فترة عملهما ٠ في هذا البحث تم معالجة المسألة الأساسية الناتجة عن تداخل الأحمال خلال عملية التحميل بأحمال المتعددة الإتساع ٠وقد تم تصميم برنامج تجريبي لجميع المعلومات حول حياة الجهاز قبل الكسر تحت ظروف (VAL) مختلفة ٠

ولمعرفة درجة وسرعة نمو الشرخ الكلالي نظريا استخدمت نظريتان ، هاتان الظريتان هما نظرية ويلرر ونظرية البرت ، وقد بنت نتائج توافق التحليل النظري مع التحليل العملى المتوفر ٠

وباستخدام المكرسكوب الإلكتروني تمت دراسة سرعة نمو الشرخ الحركي ، هذا الدراسة تسمى مراكتوترانك سنري ٠

لقد تم إستخدام المراكتوترانك سندي بنجاح لربط نمو الشرخ الحركي الظاهر بالشرخ الحركي بالمكرسكوبي ، وكانت النتائج شبه متطابقة ٠

ماجستير هندسة ميكانيكية

قسم الهندسة الميكانيكية

جامعة الملك فهد للبترول والمعادن

الظهران - المملكة العربية السعودية

يونيو ١٩٩٥

Chapter 1

Introduction

1.1 Background

Most engineering components and structures subjected to repeated fluctuating load cycling whose magnitude remain well below the fracturing load are known to fail due to the phenomenon known as *fatigue*. Fatigue is important as it is the single largest cause of failure estimated to comprise approximately ninety percent of all failures of engineering components and structures. Further more, it is catastrophic and insidious mode of failure which occurs quite suddenly.

During the past twenty years a rather extensive effort has been devoted to developing methodologies that permit the prediction of fatigue failure. As the knowledge related to the fatigue expanded, it became clear that in certain cases fatigue could

be treated from crack propagation point of view. The understanding of the crack growth behavior has led to an increase in the life of structures subjected to cyclic loads. To efficiently utilize metals one would like to avoid dealing with *fatigue crack propagation* (FCP) and final failure. However, because of performance requirements this is not always possible. Thus, a means of dealing with FCP must be devised. Predictions of how long the load must act before a critical stage is reached is a researchers principal objective.

Conventional stress-life (SN) data does not give any information about the crack length and its growth to final failure. Fracture mechanics approach provides this information. In most practical situations probability of fatigue failure is accepted for component and structures. The crack initiation part of fatigue life is essentially random but is believed to be between 1 to 10 % of total life.

Thus, where fatigue failure is by surface crack initiation and growth (which is the general case)- it is crack propagation or the crack growth process that needs to be studied for analysis. This research is an attempt to investigate the problem of fatigue from crack propagation point of view. FCP life under the *variable amplitude loading* conditions (VAL) is being presented here with emphasis on the *load interaction effect.*

The compilation of this thesis is done in the following manner;

Chapter 1 concerns the basic knowledge necessary to understand the fatigue phenomenon and its terminology. It is followed by a literature survey of the various aspects of VAL fatigue life estimate, methodologies, and phenomena observed, latter part of this chapter covers the fractographic studies reported in literature. Theoretical formulation of the fatigue life prediction models is given in chapter 3.

Different factors to be considered in the fractographic study and the interpretation of the FCP rate from the fractograph are also explained. Chapter 4 defines the outline of the apparatus to be used and other details of the test material and the experiment. The loading parameters and other relevant parameters are also defined. Calculation of FCP lives and FCG rates is presented in chapter 5. Analysis of the data is presented in chapter 6 with the final chapter commenting on the results and drawing conclusions. Some suggestions for possible future research as an extension of this research are also proposed in the end of this chapter.

1.2 Fatigue

Failures occurring under conditions of dynamic loading are called *fatigue failures.* Fatigue is a damage process in which failure occurs due to its cumulative nature, it keeps on increasing till the material can not withstand stress (strain) anymore and hence, fails. ASTM E-206 definition of fatigue is as follows;

"The process of progressive, localized, permanent structural change occurring in a material, subjected to conditions which produce fluctuating stresses and strains at some point(s) and which may culminate in cracks or complete fracture after a certain number of fluctuations."

Fatigue damage occurs in regions that deform plastically under the applied fluctuating load (stress). In general, the applied load may be axial (tensile or compressive), flexural (bending) or torsional (twisting). Thus, fatigue damage of components that are subjected to normally elastic stress fluctuations occurs at regions of stress raisers where the localized stress exceeds the yield strength of the material. Microscopically the surface is usually perpendicular to the direction of principal tensile stress. These stress raisers are usually unavoidable as they exist in the form of voids, sharp edges or notches, metallurgical discontinuities like inclusions etc.

Fatigue life of any structure or component is the number of stress (strain) cycles required to cause failure. From analysis point of view fatigue life can be classified

as *crack initiation life* and *crack propagation life* sum of which is termed as *total life*. *Crack initiation stage* is governed by the number of stress cycles required for a fatigue crack to nucleate (initiate) to become a potential stress raiser. Under the action of cyclic loading, a plastic zone (region of deformation) develops at the defect tip. This zone becomes a prospective site for a fatigue crack to grow. *Crack propagation stage* comprise of the stress cycles required to grow the initiated crack large enough to produce failure. The variables that affect fatigue include stress level, stress state, cyclic waveform, fatigue environment and metallurgical conditions of the material.

Besides above, other factors that affect the fatigue process are;

- Type of loading
- Surface finish
- Surface treatment
- Heat treatment
- Temperature
- Corrosion
- Environment etc.

1.3 Fatigue Loading

Fatigue loading can be classified on the basis of loading type. When the amplitude of dynamic loading does not vary with time the loading is termed as *constant amplitude loading* (CAL) see Fig. 1.1. Most of the base line fatigue life data is based on CAL studies. CAL serves as a good means to study the fatigue phenomenon using simplified models. The predictable nature of CAL studies makes its application very limited to the real life situations.

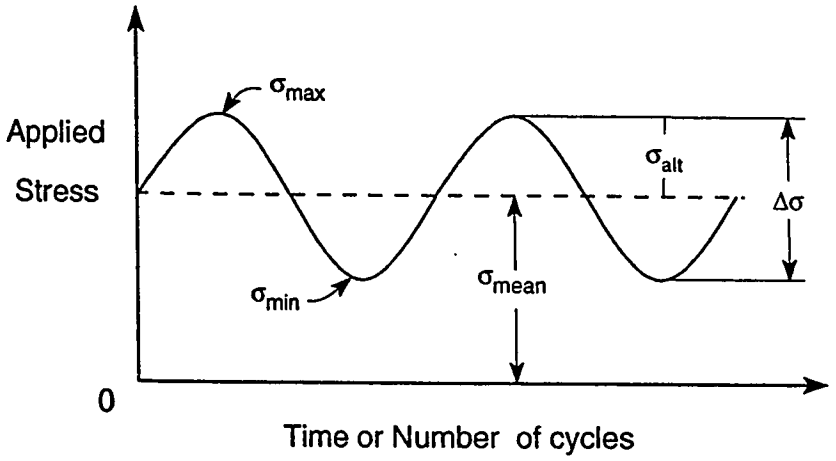

Figure 1.1: Terminologies used in fatigue loading

When the loading pattern is such that its amplitude as well as the frequency vary with time is a typical case of *variable amplitude loading* (VAL) see Fig. 1.2 (b). If the pattern of changing amplitude and frequency is random then this becomes a class

of VAL called *random loading.* This type of loading depicts the true in-service loads experienced during life of a large number of engineering components and structures such as, on aircraft structures, offshore platforms and vehicle loading on bridges etc.

Between these two extremes another class of loading can be inserted which connects different CAL loadings along with *overloads* (OL) or *underloads* (UL) or *step loading* or a sequence of different CAL steps in the form of blocks (different in frequency and/or magnitude) which are repeated to form the loading history. Such loading histories are also called the VAL type. The magnitude of stress patterns of varying degree of complexities can be accommodated in this type of loading. Such loading is more realistic than CAL and is easier to generate in laboratory conditions and analysed Fig (1.3).

1.4 Fatigue Crack Growth

Even though measures may be taken to minimize the possibility of fatigue failure, the inherent material imperfections can not be eliminated. Under the influence of cyclic stress, if unabated, such imperfections can ultimately lead to failure. The intention of a designer is to develop a criterion whereby fatigue life may be predicted on the basis of material and stress state parameters. *Fatigue Crack Growth* (FCG) is one such parameter which provides information about the resistance of a material

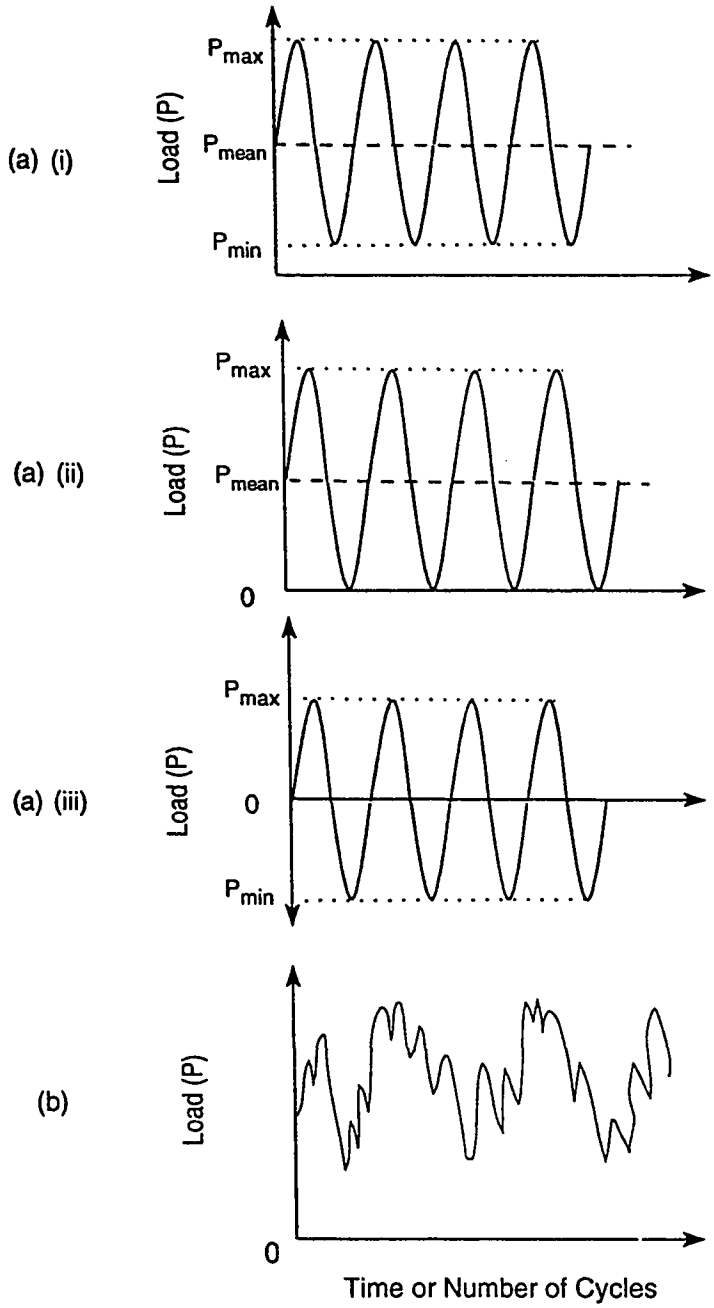

Figure 1.2: CAL with different R ratios, (a) (i) $0 \leq R \leq 1$, (ii) $R = 0$, (iii) $R = -1$, (b) random loading.

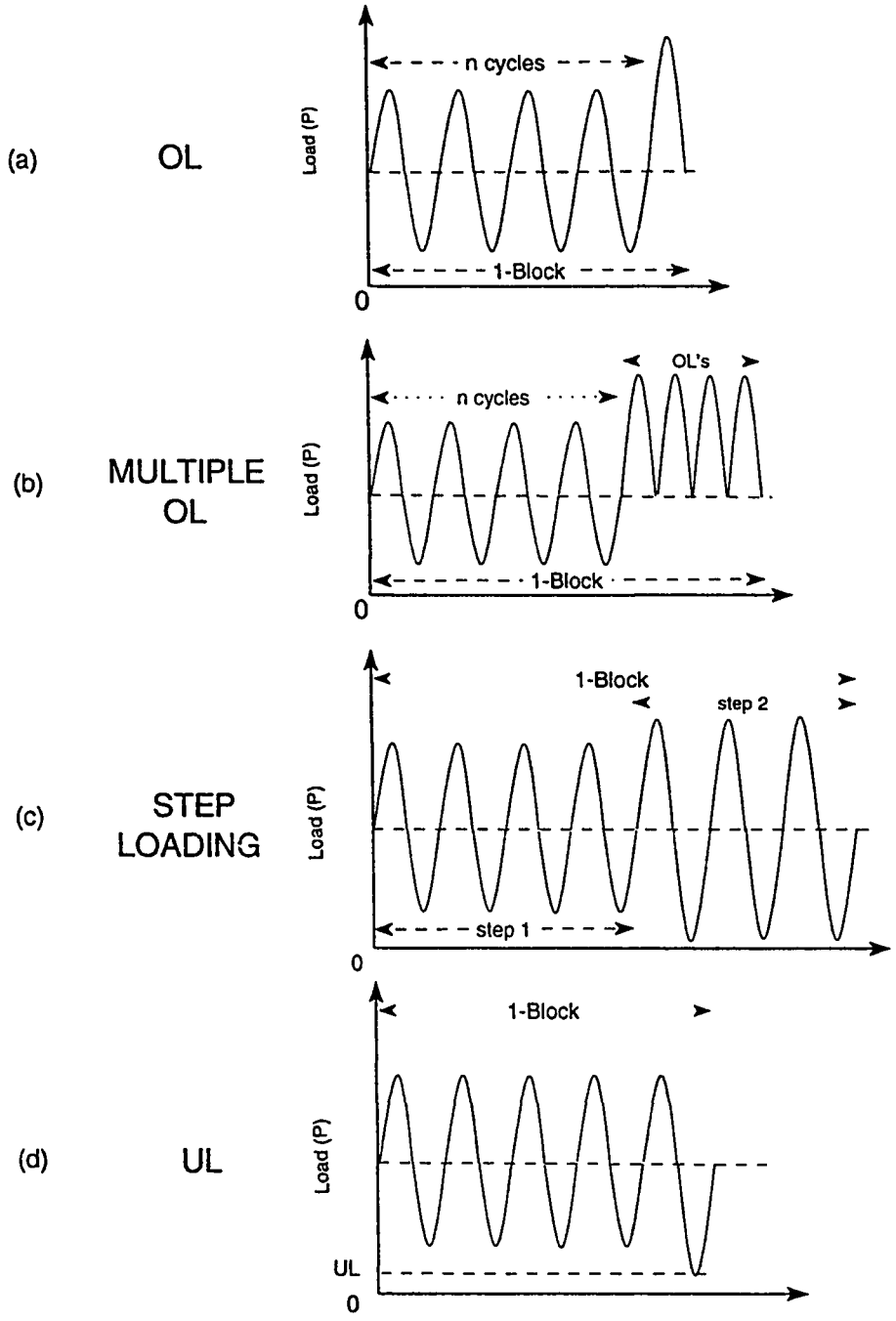

Figure 1.3: VAL history blocks (a) single OL, (b) multiple OL, (c) step loading, (d) underload (UL).

to ultimate fatigue under given conditions. Of particular interest is the crack growth rate i.e FCG rate, up until the crack attains a critical size above which catastrophic growth ensues.

Principles of *Fracture Mechanics* are employed to determine this critical size that can be tolerated without inducing failure. The method characterizes the fracture behavior in terms of material parameters that can be used directly by an analyst, such as, stress, material toughness, or flaw size. Predictions of how long the load must act before the crack reaches its ctitical size is one of the principal objectives of reaseearchers engaged in the study of FCP of materials. This information is obtained from the crack growth rate ($\frac{da}{dN}$) with units of in/cycles or m/cycles. Fatigue crack growth rate is obtained taking the slope of simple crack length 'a' vs corresponding number of fatigue cycles 'N' at each point.

FCG rate curve is plotted with *stress intensity factor range* ΔK_I on the abcissa and $\frac{da}{dN}$ on the ordinate using a log-log scale. The curve is called a *sigmodial curve* with three distinct regions see Fig. (1.4).

At low ΔK_I , **Region I**, behavior is associated with threshold value ΔK_{Ith}, effects. Below ΔK_{Ith} the cracks do not link to form large cracks. The mid region, **Region II**, is essentially linear. **Region III** is where the FCG rates are high enough

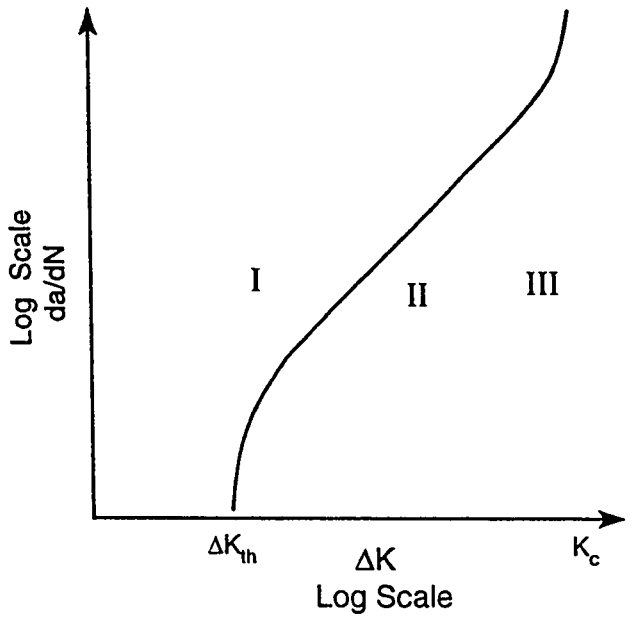

Figure 1.4: Three regions of FCG curve

to cause rapid failure and very little life is expected beyond this region.

Stress intensity factor (ΔK) is a fracture mechanics parameter that incorporates the effects in changes in crack length and the cyclic loading magnitude. It basically controls the growth of the fatigue crack during fatigue loading. It represents the driving force of the crack and is independent of the crack geometry. Fracture occurs when ΔK_I reach a critical value for the particular material. This critical value is called the *fracture toughness* of the given material. As K_I reach K_c (the fracture toughness), unstable fracture occurs. This critical value can be considered as a limiting value of K_I just as tensile yield strength $\sigma_{Y.S}$ is considered for applied stress.

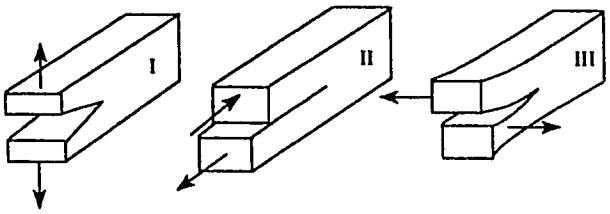

Figure 1.5: Loading Modes

Mode I used as suffices, refers to as mode of local displacement that is symmetric about horizontal axis see Fig. (1.5).

The key aspect of K_I is that it relates local stress field ahead of the crack tip in a structural member to the global (nominal) stress applied to it, away from the crack. Different relations of ΔK_I can be found in literature. The units of K_I are $MPa\sqrt{m}$ or $ksi\sqrt{in}$. Throughout the text we will use ΔK and K instead of o ΔK_I K_I, respectively.

1.5 Fatigue Crack Propagation Under VAL

It is important to note that during crack propagation, damage can be related to an observable and measurable phenomenon i.e the crack length. In CAL, fatigue

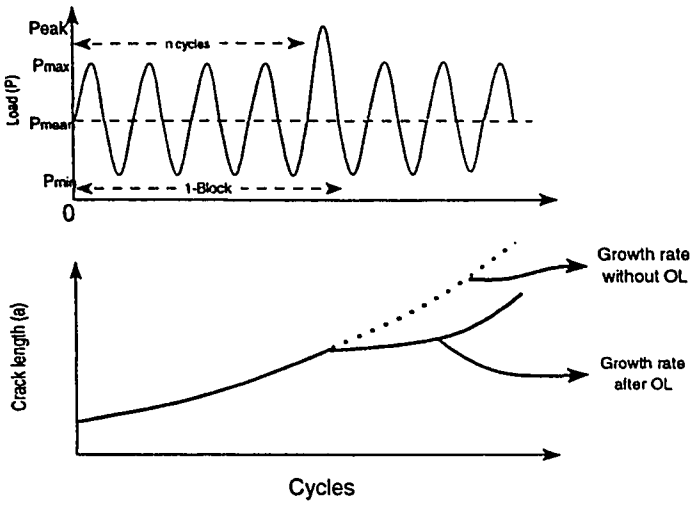

Figure 1.6: Crack growth retardation after an OL [1].

crack propagation is only dependent on present crack size and the applied load. However, under VAL conditions fatigue crack propagation is also dependent upon the preceding loading history as well. This dependence is termed as *load interaction effect* or the *sequence effect.* It is defined as deviations of the actual crack growth rate per cycle under VAL history from crack growth rate as predicted on the basis of constant amplitude crack growth data.

The consequence of this effect may be observed as *retardation* or *acceleration* or *arresting* of the growing crack. Hence, load interaction significantly affects the FCG rate and consequently the fatigue life Fig. (1.6). Even the application of single tensile overload (OL) within a CAL block can produce a marked retardation in the

FCG rate. Crack retardation remains in effect for a period of loading after the OL. The number of cycles in this period has been shown to correspond to the plastic zone size developed due to the OL (see sec. 1.5.1). Number of cycles in the CAL block, the OL and the UL stress magnitude affect the FCP lives [2].

If the OL magnitude is large enough the growth temporarily stops. This phenomenon is called *crack arrest* [3]. The OL produces a new larger plastic zone at the the crack tip responsible for the arresting of the growing crack.

1.5.1 Plastic Zone

On the application of an OL, the material develops plastic strains ahead of the crack tip. This happens because the yield stress in the region near the crack tip exceeds the tensile yield strength of the material. The amount of plastic deformation is restricted by the surrounding material, which remains elastic. The size of the plastic zone is dependent on the stress state of the body.

Under plane stress conditions the plastic zone size for cyclic loading is given by;

$$r_y = \frac{1}{\beta\pi}\left(\frac{K_c}{\sigma_{Y.S}}\right)^2 \qquad \textit{for cyclic loading} \tag{1.1}$$

where $\sigma_{Y.S}$ is the tensile yield strength, β is 2 for plane stress, 6 for plane strain conditions and K_c is the fracture toughness of the material used .

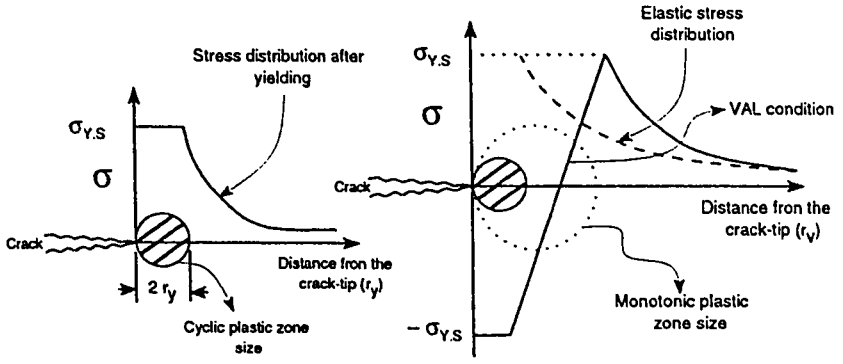

Figure 1.7: Plastic zone ahead of the crack [1].

Application of OL takes the crack-tip material beyond the yield point, a plastic zone is formed in the region of the crack-tip Fig. (1.7). On the UL (unloading part of the cycle), residual tensile stress field is created. When subsequent loading cycles are applied, residual tensile stress varies in cyclic manner causing earlier crack opening until the crack-tip approaches the boundary of the residual stress field (also see Fig. (3.1). Effect of UL dose not last long as that of OL.

1.5.2 Residual Stress

Residual stresses due to strain hardening are usually left in a material which has undergone plastic deformation during machining or joining processes. If such stresses

are tensile in nature, they can promote fatigue cracking and decrease fatigue life (depending on the magnitude and orientation), therefore tensile residual stresses are avoided in any material that is subjected to fatigue conditions. On the other hand compressive residual stresses tend to increase fatigue life [4].

After each OL cycle in a VAL block, a plastic zone is created in the crack path. This zone undergoes a compression by the surrounding elastic material and produces a compressive *residual stress* at the crack tip. This effect causes *blunting* of the crack tip front and results in crack retardation. This effect is even more pronounced with the increase in magnitude and the duration of the OL ratio defined by $\frac{K_{OL}}{K_{max}}$; a term of interest in the analysis of FCG rates.

1.5.3 Crack Closure Effect

Crack closure is a term usually used for explaining the R ratio effect of crack growth rates as well as environmental effects on ΔK_{th}. The fatigue crack is fully open only for only a part of the load cycle, even when the cycle is fully in tension. This phenomenon is the direct consequence of the permanent tensile plastic deformation left in the wake of the propagating crack making the mating surfaces incompatible. It was observed that the surfaces of the fatigue crack close (contact each other) when the remote load is still tensile and do not open again until a sufficiently high tensile load is attained in the next cycle.

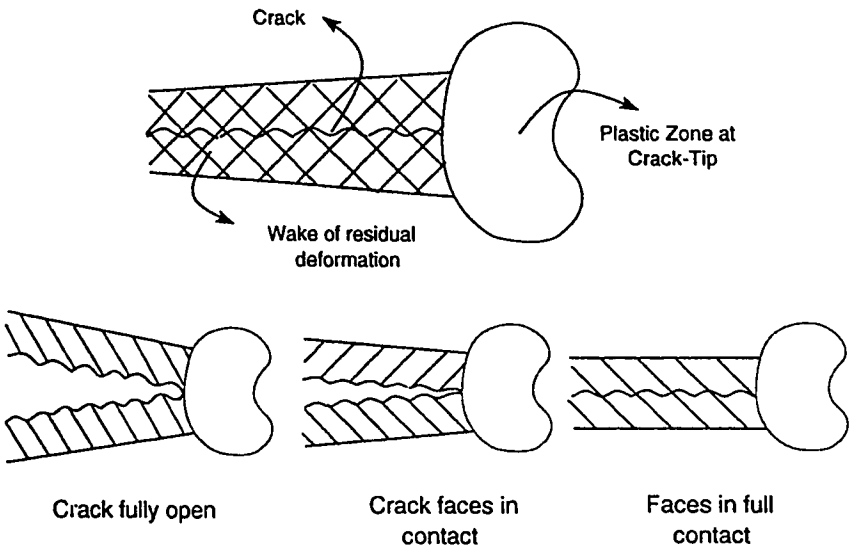

Figure 1.8: Crack closure phenomenon with plastic zone effect

Elber described the crack closure phenomenon as a result of crack-tip plasticity. A plastic zone develops around the crack tip as the tensile yield stress of the material is exceeded. As the crack grows, a wake of plastically deformed material is developed while the surrounding body remains elastic see Fig. 1.8. He proposed the idea of crack opening stress, saying that it was the value of applied stress at which the crack is just fully open σ_{OP}. Part of the interaction effect could be explained by this phenomenon. Crack closure is measured by *compliance method* or *electrical potential drop method* by most of the researchers [5].

1.6 Current Status of The Problem

During the past twenty five years extensive effort has been devoted for developing methodologies that permit the prediction of fatigue lives by different analytical models. Since crack like defects or discontinuities such as voids, inclusions, geometric stress raisers and weld defects are inherently present in a given structure, the crack initiation portion of the total fatigue life becomes less significant than the crack propagation portion. In such situations the study fatigue crack propagation becomes the primary concern. From a good understanding of the FCG behavior it is possible to extend the useful service life and predict failure. Hence, FCP is an important tool from design as well as service point of view of component and structures subjected to cyclic loading.

Almost all engineering structures and components are subjected to VAL cycling. Literature survey shows that most of the previous work done by researchers is based on CAL. Prediction models have to satisfy criterion which determines their ability to predict the fatigue life under various load histories and to consider the material behavior with the mechanistic aspect of fatigue. Hence, presently available fatigue life prediction concepts require not only the baseline CAL data, but additionally VAL data is needed to arrive at reliable fatigue life predictions with reasonable accuracies.

Of particular interest is the study of crack growth under VAL with OL and UL with the realization of the fact that FCG can comprise significant portion of the life of a critically loaded engineering components or structure. In addition, the treatment of this subject has been advanced by developments in the field of Fracture Mechanics. Later, the introduction of *servohydraulic testing systems*, and the availability of *Transmission Electron Microscope (TEM)* and *Scanning Electron Microscope (SEM)* for fractographic examination of the fracture surfaces has opened new horizons for research.

Some controversial issues are reported in the findings of single overload applied in a VAL loading history [6]. A group of researchers report that retardation increase with increase in the baseline loading range ΔK, for a given overload ratio [7, 8, 9]. While another group observed that retardation decrease with increase in base line loading range for similar conditions [10, 11, 12]. This is a puzzling point reflecting the characteristic difficulties of a single OL, which has became the source of interest for this study.

1.7 Scope of Present Work

The ultimate goal in material science is for producing materials with good mechanical properties, good corrosion and crack growth resistant properties which are all

possible to achieve in a single material. When fatigue is the determining factor in design, then, prediction of how long the load must act before fracture is reached is the question which is answered by knowledge of fatigue crack growth behavior of a given material.

Crack growth predictions are most often used in aircraft industry, in particular to prove the damage tolerance of structure to determine approximate inspection intervals. Such work can be of significant help to the designer in extending the life of structures, improving the utilization of material, selection of process steps, establishing inspection controls and analysis of failure.

The purpose of this research is to investigate and apply the current knowledge of FCP concepts as a design and material selection tool. The literature survey shows that mostly aluminum and steels were used for most of the investigations. Infact more than seventy five percent of the literature explored showed aluminum as the material of study, although the significance of steels was not denied. As steels are still considered to be the primary structural and component source, we have selected stainless steel for this investigation.

Due to the complex nature of single tensile overload application in VAL, this investigation will be concentrated in that direction. As already mentioned, that

FCP life is more important than life the entire fatigue life, so we shall concentrate on FCP life only.

Two analytical models namely the Wheeler's model and Elber's model applicable to VAL will be applied to predict the FCP life. Paris and modified Paris equations will be used in the Wheeler's model. Physical measurement of fatigue striations will also be used to obtain FCP rates. A comparison of fatigue lives will be made between the experimental and theoretical findings.

Chapter 2

Literature Review

Most of the analytical approaches to the fatigue problem have attempted to relate the crack growth rate with the crack length, plastic enclave size, material constants, stress and specimen geometry. The relationships differ primarily in emphasis placed on the variables and the concomitant assumptions.

One of the basic differential equation governing any fatigue study is given by Paris and Erdgon [13]. Their study relates crack propagation with the range of stress intensity ΔK. Later studies have shown that it only applies to the region II of the FCG rate curve for only CAL loading. Many FCP laws have been listed by Hoeppner and Krupp [14] involving different material and empirical constants. Factors that restrict the use of one model over the other have also been discussed.

Different OL stress intensity to the maximum stress intensity ratios ($\frac{K_{OL}}{K_{max}}$) which are followed by CAL cycles have shown no retardation up to a ratio of 1.2, and a temporary crack arrest at a ratio of 1.6 [15]. Crack opening stress has been used to explain this effect. Fatigue problem of high-low loading cycle has been tackled using a stochastic model [16]. A nonlinear damage parameter D is used in addition to the randomness of the material parameters giving good agreement with the experimental results by McEvily [17]. Interaction effects following OL is explained using the *crack closure* theory, with stress ratios and microstructure also shown to have effect on FCG rate.

Forman [18] incorporated crack instability at the onset of fracture (fracture toughness) and stress ratio into the paris equation to obtain its modified version applicable to VAL with satisfactory results. Misawa reports that number of cycles in the CAL block and the OL and UL stress magnitude effect the FCP lives [2]. With number of UL stress cycles increased, the propagation rate decreased and then the crack stopped its propagation (crack arrest). Schwalbe [19] has compared different FCP models with experiments performed on four materials proposing the possibility of presenting equivalent crack propagation models based on different assumptions. Young's modulus, mean stress and stress intensity factor are reported to be most important parameters regarding FCP rate.

A general overview of different methodologies that were presented over the past few years have been critically reviewed by Heuler and Schutz [20] in which Wheeler's model is reported to give good results. Limited data on the effect of thickness on retardation following OL suggests the retardation decrease as the section thickness increases, which implies that the effect is primarily a plane stress phenomenon [21]. Hua and Socie [22] reports that fatigue lives under VAL can be predicted from CAL damage curves if a single type of crack system dominates the fatigue process. Under random loading, the Wheeler's model is used in conjunction with simulated results of the stochastic model developed by Alawi [23]. The results of this probabalistic model are conservative in estimating fatigue life without considering the retardation effect (i.e. shapping parameter $p = 0$). On another occasion under VAL when tensile OL was applied frequently, no acceleration or retardation in crack propagation rate was observed by Masuda [24]. While acceleration was reported when the UL was applied. Steels were reported to show little effect of change in frequency below $\Delta K < 10MPa\sqrt{m}$.

Different VAL loading patterns investigated showed that retardation effect due to OL was decreased if low loads were applied immediately after the OLs by Marrisen [25]. Further, more than one peak of OL causes more damage, and combine effect of step loading (fifty cycles in each step) is almost same as that of CAL of the low loading level.

The literature survey carried out for this study is being presented under seven different categories as under;

2.1 Fatigue Life Prediction For VAL Histories

Different attempts have been made to tackle the fatigue problem. All initial attempts were made on CAL due to restricted information of the subject and other technical reasons. Since components and structures are mostly subjected to VAL there is a need to correlate the CAL research to VAL.

A comprehensive report on how to collect data, report, and calculate fatigue life for CAL has been given by Richard et. al. [26]. Crack growth measurements from different sources were used to compare the effects of R values and cyclic frequency under CAL of aluminum alloys reporting in crack growth rate with higher frequencies (especially in dehydrated air). Others report metallurgical factors to affect FCG rate quoted by Hahn [27]. Studies carried out by Bilir and Kyurek show that without the interaction effect the FCP life estimates were within the acceptable limits [28]. Johnson et. al. [29] has shown that the case of impact loading cannot be predicted by CAL methodologies and suggested a VAL approach to be followed.

Porter [30] used a reduction factor to normalize the CAL data for same K levels to predict and correlate FCG rate trends. The effect of repeated OL, block size and peak stress levels was studied to report fair agreement with the experimental data, though for some cases the error was quite large. Five different CAL models were studied by Solin [31] to be modified as equivalent models for VAL. Good correlation was reported for spectrum loading (with no interaction effect). Same has been done for steels taking different R ratios and frequencies into account [32]. Other contributions in this direction are also reported in literature [33].

Some RMS equivalent models of FCG for VAL were presented by Sonsino reporting good agreement with SN curves for very few cases [34]. Equivalent CAL concept was also shown to be applicable in cases of short stationary loading also by Gabra and Bathias [35].

Different FCG models were surveyed by Hoeppner and Krupp [14] and by McEvily [36]. Linear summation rule of crack growth based on the cyclic J-integral method has also been used for FCG rate under VAL [37]. Other VAL models are also reported elsewhere [38, 39, 40]. Three different methodologies for estimation of FCG life show that very high spectrum loads result in under estimation of fatigue life when interaction effect was considered rendering them unsuitable for cracks with small initial sizes [28].

A new damage parameter based on net effective strain was developed by DuQuesnay et. al. to predict the total life. The evaluation of this parameter was not easy [41]. Pippan [42] suggested that under VAL no single value of ΔK_{th} be used, instead, a curve between R ratio and ΔK_{th} was recommended.

2.2 Retardation Models

A comprehensive view of the retardation phenomenon was presented by Packman [43]. Peak loads were found to cause retardation of crack growth rate which became stronger with the increase in the peak to baseline stress ratio or decrease with decreasing peak to baseline stress intensity range, while multiple OL resulted in additional retardation. Retardation was reported by Tanaka et. al. to increase with the material constant m [44]. The steep increase in retardation with the decrease in baseline ΔK was related to threshold of stress intensity of the material.

In crystalline alloys, increase in the R ratio accelerated near threshold crack growth rates and decreased the value of ΔK_{th}. This effect of R becomes more prominent when its value was raised from 0.1 to 0.5 . Alpas reports that in metallic glass this effect was completely opposite [45].

Studies in high strength steels show that under block loading, retardation of the crack growth rates could be correlated to the post OL retardation caused by residual stresses [46]. The distribution and the magnitude of the residual stress was not affected by the envoirment. For some materials a loading change from negative R to positive R resulted in producing a retardation transient [47]. While Shih and Wei [48] concluded their research by reporting the interaction effect can not be explained by crack closure concept alone for VAL histories.

2.3 Retardation Due To Single Tensile OL

Single tensile overload (termed as OL) is the primitive building block of the VAL and represents the simplest situation involving retardation. Thus, the response of the material to OL must be understood well enough for more realistic modelling of random load fatigue. General agreement exists on the following features;

- the magnitude of OL is most effective factor in calculating the length of retardation.
- materials with low yield strength display more retardation. [49]
- retardation decreases with increase in section thickness.

Single OL was reported to cause initial transient acceleration and then retardation in crack growth rate. The distance effected by the retardation was found to be

generally longer than the size of the OL plastic zone size. High-low sequence were also reported to cause retardation by the same authors.

Ohrloff [50] reports that single peak OL showed higher crack propagation rate immediately after the OL but then dropped considerably. The equilibrium CAL rate only reached after the crack had propagated several hundred microunits away from the position of OL. Further, even higher propagation rates were observed for periodic OL and UL combinations if they followed each other after a relatively few numbers of baseline cycles.

Acceleration in crack growth rates has been reported by Nosho [51] for cases where very small number of cycles (e.g 2) of over stress were applied intermittently between very large (e.g 10^6 cycles) of understress below the ΔK_{th}. Ogura and Ohji [52] have also studied single OL and step loading using FEM technique. The characteristic behavior was explained in terms of residual stress which had been induced by OL or a load preceding to the variation. The analytical (FEM) and the experimental results were reported to be consistent.

Jones has reported that strain hardening had little if any effect on FCG rate after OL [53]. Percentage of OL was used by the author as an indicator of the amount of subsequent retardation. He reports that crack growth after peak OL was

characterized to have effect after twenty percent OL, arrest immediately followed after seventy and 100 percent OL. No retardation was reported after fifty percent OL.

A new model for FCG retardation resulting from applied OL was determined using the concept of residual stress due to plastic deformation which reduces the value of ΔK that drives the FCP. This information is used to define and quantify an effective ΔK_{eff} that applies during the retardation period [54]. Predictions obtained from this model exhibit the delayed retardation effect and other experimentally observed features of OL influenced FCG rate.

On one occasion single tensile OL test showed that the number of delay cycles caused by one peak was between 9000 to 9500 cycles. Delay observations resulting from two single peaks OL gave greater number of delay cycles. Further, maximum interaction between two single or block OL study was found useful as it led to significant increase in the fatigue life of components by proper positioning of the peak loads have been reported by Mills.

UL after an OL can significantly decrease the crack growth delay of the latter . This study reports that crack retardations were not only controlled by the last high peak that occurs in the sequence but also by preceding peak loads (OL) [55]. The assumption that high R ratio and load sequence effects were not valid for a VAL

were also rejected by the authors.

It is also reported that high magnitude of OL have an acceleration effect followed by a prolonged retardation before the crack growth returns to the baseline levels. The extent of delay increase with magnitude of OL. At near threshold levels complete arrest of crack advance occurs. Compressive residual stress in the OL plastic zone and crack closure were reported to be the cause resulting in wedging of the mating surfaces, producing retardation. Isolated OL have also been found to cause retardation but generally under random loading crack appeared to keep propagating [56].

Retardation was considered to be controlled by parameters like, rate of crack OL and its intensity, number of OL cycles and their frequency. Crack length affected by retardation depended not only on plastic zone size geometry but on residual compressive stress it entails. Higher the frequency and magnitude of OL, higher is the retardation [57]. Thomas showed that although both the number of delay cycles and the extent of delay zone size are functions of the applied VAL, the basic shape of the relation between the crack length and the applied cycles retains the characteristic shape. There was some scatter in all cases which was probably due to the envoirmental variations [58].

Zhang has predicted FCG under VAL considering OL, UL and combinations of both OL and UL solving the modified Paris equation (with ΔK_{eff}) numerically, with good agreement with the experimental results [59]. He reported that the OL causes the crack growth rate to become slow.

Packman observed that retardation increase with high value of peak stress for a constant value of lower stress level, retardation was minimum where compression (UL) was applied immediately after the OL. UL ($R = -1$) substantially increased the FCG rate, no effect with $R > 0$ and low-high sequence having no effect at higher load levels was reported [43]. On the other hand, Porter reports that single OL produced a retardation of crack growth by an order of magnitude, and an increase in R ratio increased the FCG rate [30].

2.4 Acceleration Due To Single UL

As the crack is pressed to remain closed in the positive portion of the loading cycle, the effect of compression cycle had long been considered minimal. Periodic UL can significantly accelerate the near threshold crack growth rates, specially by reinitiating the growth of long fatigue crack previously arrested at ΔK_{th} or by reducing the fatigue crack threshold [60, 61, 62], a behavior associated with diminished levels of crack-tip shielding resulting from decrease in residual compressive stress in the

plastic zone.

Zhang has reported that UL when compared with CA showed crack surface open earlier immediately after compression causing a increase in ΔK_{eff} (decrease in σ_{OP}) thus, increasing the FCG rate. While OL and UL sequence caused retardation to the OL induced retardation effect.

Periodic FCP was reported to accelerate significantly by under stressing below ΔK_{th}, even more acceleration in low strength materials (steels) [63]. Acceleration in FCP rate as a function of frequency and envoirment has also been reported [14]. As frequency of loading was decreased, FCP rate increased by order of $2-5$ times in limited ΔK range. Periodic UL were also reported to produce acceleration with a tendency of a decreasing effect with increased number of intermediate baseline cycles [50].

2.5 Crack Closure

Pioneer of the crack closure phenomenon was Elber [64, 65], who proposed the idea of the crack propagation, only during the tensile portion of the cycle while in the compressive portion it is assumed to be closed and hence not propagating. This idle portion of crack growth was the cause of retardation according to Elber. Zhang has

analysed the effect of OL, UL and their combination using crack closure through quantitative description of influence on stress and crack opening displacement [55]. OL caused large plastic zone infront of the crack-tip indicating that the crack closure takes place much earlier for the immediate loading cycle following the OL. Consequently, the crack opening stress σ_{OP} is higher and the crack growth is hence lower. In subsequent CA part of the block, the crack-tip continues to grow through the large plastic zone with retarded plastic zone left far behind the crack-tip.

Shih and Wei have reported crack closure even for $R < 0.3$ using electrical potential method and measuring the crack opening displacement and strain measurements [48]. They concluded that onset of closure depended upon R and K_{max} and that it was not the only phenomenon to fully understand the interaction effect. Alpas et. al. also observed crack closure at low R ratios but they could not explain the inverse R ratio effect [45]. For higher R ratios they have proposed a crack growth model to account for the crack face buckling which obscured the effect of closure.

2.6 Fractography

A typical electron fractograph show well defined striations which can be related to the FCG rate. Utilizing striation count on the fractograph, the crack growth rate ($\frac{da}{dN}$) can be evaluated to determine the basic stress intensity level applied to the

specimen, if the baseline FCG information is available for the conditions of interest [14].

Under the normal zero-degree angles of observations the area covered by the micrograph is more or less featureless. Only on a small plateau will ill-defined striations can be observed specially for steels. Fracture surface in steels generally show ill defined striations, if any, while for other materials striations may be visible over 40% of the surface [66]. The striations usually are narrow, fine and so short that it is difficult to obtain a good resolution [67].

A fairly large scatter in measurements occurred mainly because of scatter on general and also because of scatter of the local inclination of the crack surface. A correction of the microscopic measurements was applied to correlate with the macroscopic crack growth by multiplying by a factor [68]. As a result striation spacing during the OL block remained practically constant with no systematic variation of spacing during both the UL block and low amplitude block.

Wang et. al. used $50X$ *to* $3500X$ magnifications to monitor steel samples perpendicular to the electron beam. For VAL fatigue crack growth regions were much more irregular than CAL and striations were fewer, more poorly defined and difficult to locate [69]. In some cases a form of striationless FCP was observed suggesting

dependence on number of applications of peak stress. Dependance on frequency and was also reported showing that the striations spacing increased with decreasing frequency and increased with increasing stress intensity factor [70].

Chapter 3

Analytical Formulation

Fatigue crack propagation under variable amplitude loading is significantly influenced by the preceeding load cycles (the interaction effect). So, the constant amplitude loading models can not provide satisfactory estimates of the fatigue lives of components in actual service conditions. New models to incorporate the load interaction effect have to be used to predict fatigue crack propagation lives, or even total lives for that matter, under VAL history. Linear Elastic Fracture Mechanics principals are used to relate stress magnitude and distribution near the crack tip to the remote stress applied to the cracked component, the crack size and shape, and the material properties of the cracked component.

As discussed earlier, in a large number of situations, fatigue life propagation can constitute over 90 percent of the total fatigue life, and thus the main focus of the

present investigation will be placed on the fatigue crack propagation studies. It can then be safely assumed that in such situations the component either already contains a crack or a crack like defect of sufficient size or rapidly develop a crack in the early stage of the fatigue life.

As the emphasis of this investigation is mainly on FCP, we can exclude the fatigue crack initiation life study and concentrate on the FCP part of the total life. FCP constitutes the portion of life spent in growing a predominant crack size to unstable length where final fracture takes place. In order to distinguish between the crack initiation and propagation lives, the specimen were pre-cracked to 0.001 m as the initial crack length 'a_i'. Growth of crack from this length will be monitored till the final length 'a_f' and recorded as fatigue life data.

Fatigue lives of a critically loaded part are conservatively predicted by integration of a relationship describing the crack growth rate as a function of mechanical crack driving force, from initial to final crack size. For nominally linearly elastic conditions, when driving force can be defined interms of the applied ΔK. This relation is given by Paris equation (3.1).

3.1 The Wheeler's Model

Different models have been proposed to deal with the VAL conditions using as a baseline CAL data. *Crack-tip plasticity* model is one of them. It links the sharpness of the crack-tip with the crack retardation. Crack-tip blunting is proposed to occur as a result of the OL. The stress concentration associated with the crack becomes less severe, resulting in slowing down of the crack growth rate. A large plastic zone develops during the OL. The interaction effect (retardation) persists as long as the crack-tip plastic zones which develop on the following cycle remain within the plastic zone of the OL. One model which describes FCG rate in the light of crack-tip plasticity is the Wheeler's model which is described below.

Wheeler's model predicts that retardation in the crack growth rate following an OL under VAL conditions may be predicted by modifying the CAL growth rate. This means that already existing FCG rate model developed for CAL studies can be used by incorporating a factor dependent on the interaction effect. Unfortunately, this requires a *shaping parameter 'p'*, which has to be obtained experimentally for different materials.

To start with, the basic governing differential equation followed is the Paris equation [13];

$$\frac{da}{dN} = C\ (\Delta K)^m \tag{3.1}$$

where, C and m are material constants. To obtain these constants crack length vs cycles to failure is plotted in Fig. (5.1). The slope of the a vs N curve is obtained at each point i.e $(\frac{da}{dN})$. Now, for an elliptic notch, the stress intensity factor using fracture mechanics concept is given as;

$$\Delta K = f(g)\ \Delta\sigma\ \sqrt{\pi\ a} \tag{3.2}$$

where, $f(g)$ is a geometric correction parameter [71, 48] whose value lies generally between 1 to 1.4 [1]. It depends upon the specimen (finite width effect, front wall effect etc.) and crack geometry (elliptical, circular. semi circular etc.). Any error in its evaluation may be very small compared to the uncertainties of the fatigue process [1]. $\Delta\sigma$ is the global stress range (MPa). a is the instantaneous crack length. According to Wheeler's model [72], equation (3.1) can be written in terms of constant amplitude growth rate with a retardation parameter C_p as;

$$\frac{da}{dN_i} = (C_p)_i\ (\frac{da}{dN})_{CAi} \tag{3.3}$$

where, $(\frac{da}{dN})_{CAi}$ is a constant amplitude growth rate approximated by the stress intensity factor range ΔK_i, the retardation parameter $(C_p)_i$ is a function of the ratio of current plastic zone size to the plastic zone size created by the OL, given by;

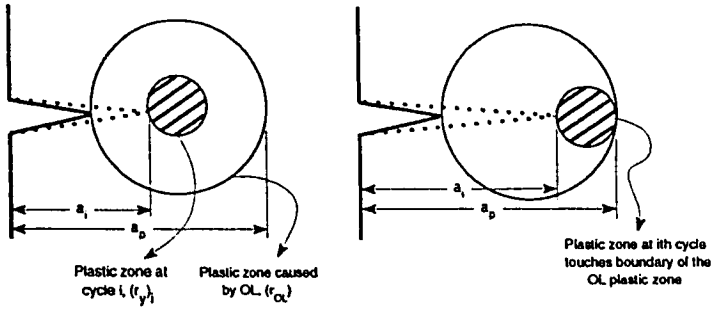

Figure 3.1: Plastic zone parameters used in Wheeler's model.

$$(C_p)_i = \left(\frac{r_{yi}}{a_p - a_i}\right)^p \tag{3.4}$$

where, r_{yi} is the cyclic plastic zone size due to the i^{th} loading cycle (see section 1.5.1 and Fig. 1.8), p is an empirically determined shaping parameter, a_i is the crack length at the ith loading cycle and a_p is the sum of the crack length at which the OL occurred and the OL plastic zone size given by: $(a_p - a_i) = a_o - a_i = a_i + r_{OL} - a_i$. Assuming that the crack length just before the OL is relatively close to the crack length at which OL occurred, then, $a_p \simeq r_{OL}$ [1, 73]. This corresponds to assuming that $(Cp)_i \simeq Cp$, where Cp is the average value. A graphical representation these terms is given in Fig. (3.1).

According to the wheeler model, retardation decreases proportionally to the

penetration of the crack into the OL zone with maximum retardation occurring immediately after the OL. The value of $(C_p)_i$ range from 0.0 to 1.0. Crack retardation is assumed to occur as long as the current plastic zone size is within the plastic zone created by the OL. As soon as the boundary of the current plastic zone touches the boundary of the OL zone, retardation is assumed to cease which corresponds to $(C_p)_i = 1.0$, and the retardation is maximum at $(C_p)_i = 0$.

3.1.1 Paris Equation

In equation 3.3, the constant amplitude crack growth rate can be found using Paris relation equation (3.1) and the stress intensity factor given by equation (3.2). The integration of this crack growth equation with reference to the crack length a yields the theoretical value of fatigue crack propagation life (N_p) as predicted by the Wheeler's model using the Paris equation given by;

$$N_p = \int_{a_i}^{a_f} \frac{1}{(C_p)^p\, C\ \ (f(g)\ \Delta\sigma\sqrt{\pi\ a}\ )^m}\ da \tag{3.5}$$

where, a_i is the initial (precracking) crack length, a_f is the final fracture crack length given by;

$$a_f = \frac{w}{2} - \frac{P_{max}}{2\ t\ \sigma_{Y.S}} \tag{3.6}$$

with w as the width of the specimen, t as the specimen thickness and P_{max} as

the maximum load applied during the constant amplitude part of the cycle.

3.1.2 Modified Paris Equation

Allen [56] has reported steels under VAL to be influenced by the stress ratio R. In equation (3.3) the CAL relation given by Paris was modified by;

$$\frac{da}{dN} = \frac{1+R}{1-R}\, C\, (\Delta K)^m \tag{3.7}$$

where, C and m are the paris constants found by the constant amplitude loading test, R is the stress ratio given by; $(\sigma_{min}/\sigma_{max})$ and ΔK is given by equation (3.2).

The integration of equation (3.7) (with a_f same as 3.6), will yield the predicted fatigue crack propagation life using Wheeler's equation as;

$$N_p = \int_{a_i}^{a_f} \frac{(1-R)/(1+R)}{(C_p)^p\, C\, (\Delta K)^m}\, da \tag{3.8}$$

3.2 Elber's Model

Elber's model [65] presented FCG rate model under VAL utilizing the compressive residual stress at the crack-tip to predict FCG rate. Stresses are developed due to the elastic body surrounding the OL plastic zone, which causes these zones to go into compression after removal of the OL. The crack is assumed to propagate in the

tensile portion of the cycle and in the compressive portion, it assumed to be closed and not propagating.

The basic crack growth rate equation (3.1) can be same as the one used by Paris with some modifications to accommodate the effective stress concept. Hence, the required effective stress intensity range (ΔK_{eff}) is given by;

$$\Delta K_{eff} = U\ \Delta K \tag{3.9}$$

Though U may be taken a complicated function varying from cycle to cycle and from one loading condition to another, but for conventional fatigue program U can be assumed to be quite simple and a function of R only [25].

where,

$$U = 0.618 + 0.365R + 0.139R^2$$

The above effective stress relation was incorporated by Marrissen in order to account for the crack opening behavior using ΔK_{eff} (equation 3.9). This relation was obtained from the data by linear regression for $0 \leq R$ which is satisfied by our loading conditions as well. Many authors have used this and similar relations to give satisfactory results close to the experimental findings [48, 50].

Using the above relations in equation (3.1) the FCP lives from Elber's model can be calculated as follows;

$$N_p = \int_{a_i}^{a_f} \frac{1}{C\,(U\,\Delta K)^m}\,da \tag{3.10}$$

$$N_p = \int_{a_i}^{a_f} \frac{1}{C\,(0.618 + 0.365R + 0.139R^2)\,\Delta K)^m}\,da \tag{3.11}$$

3.3 FCG rate From Fractograph

As already mentioned that fatigue striations are the traces of a crack advancing in each cycle [19, 74] and that they can be used to predict FCG rate. We can use these fractographs to obtain the FCG rate by physically measuring the distance between striations.

A fractograph is a thousands of times blownup view of a fractured surface. A typical fractograph should have clear well defined striations. Knowing the number of striations in a unit length of a fractograph along with the magnification used can be used to get the FCG rate [14];

$$\frac{da}{dN} = \frac{1}{Magni.} \times \frac{distance\ on\ the\ fractograph}{striation\ count/unit\ distance\ on\ the\ fractograph} \tag{3.12}$$

As many points as possible, should be obtained from each sample, all along the fractured surface in order to get the true representative FCG rate to be compared with any reference (experimental or any other source). In addition, their respective distances from the reference point (i.e the notch) will determine the crack length a_i. With this information one should be able to calculate the FCG rate using the above equation and the stress intensity range from equation (3.2). These values are plotted against the FCG rate and ΔK values of the optical findings obtained from experimental data shown in chapter 6. This will give a means of comparison between the two. Such a comparison is given in chapter 6.

Chapter 4

Experimental Setup And Collection of Data

The experimental program conducted for this investigation can be divided into five parts. First part consists of the nomenclature and setting of the testing equipment. The second, discusses material selection, notch geometry and specimen preparation technique. The third part covers the design and VAL history generation using FLAPS. This is the most important part of the whole program. Fourth part sheds light on how to collect and record the fatigue life data in raw form i.e $'a'$ vs $'N'$. Fifth and the last part covers how to examine the fracture surface on SEM, and to obtain clear enough fractograph to be able to count fatigue striations. Details of each part are as follows;

4.1 Testing Apparatus

The apparatus used in order to obtain fatigue crack propagation lives falls into three categories.

- Instron 8501, Fatigue Testing System
- Questar QM-100, Microscope and Recorder
- Joel *JSM* T-300, Scanning Electron Microscope

4.1.1 Instron 8501

A closed loop servo-hydraulic, dynamic, single axis fatigue testing system was used to generate and design VAL as well as CAL histories. The main controlling modes of the system were strain, load ($\pm 100KN$) and position ($\pm 75mm$) with a frequency range of 0 *to* 200 Hz. The controlling limits could be viewed on the digital control panel any time during the test along with any other test variable (e.g. maximum/minimum limits of each cycle or the safety limits set or number of cycles or the time elapsed).

CAL required for pre-cracking the specimen was generated from the digital control panel provided with the Instron system. Different waveforms like ramp, sine, trapezoidal, triangular, square or random loading could also be generated. Besides

CAL, different combinations of these waveforms i.e VAL histories, in the form of blocks could also be generated using FLAPS.

The specimen is held in the jaws of the load and the actuator cells. After clamping one end (the actuator end) of the specimen , second end is clamped making sure that the alignment is correct by slowly lowering down the load cell. Any pre-tension or compression induced during mounting or clamping is then removed by re-calibration of the load cell. Now the specimen is assumed ready for testing in either CAl or VAL mode. A view of the whole system is shown in Fig. (4.1).

4.1.2 Questar QM-100

Different crack measuring techniques are given by Frost and Marsh [5] which include Direct current potential difference method, non destructive testing using A.C field measurement, ultrasonic method, acoustic methods. SEM by steroimmaging, laser inferomery and optical microscope.

The equipment we have used was optical type for its simplicity, easy operation, versatility and compactness. It consisted of a horizontal travelling microscope, QM-100. The crack is observed through the vertical opening during the testing. Photographs can be captured at the same time through the axial opening where a camera can be mounted .

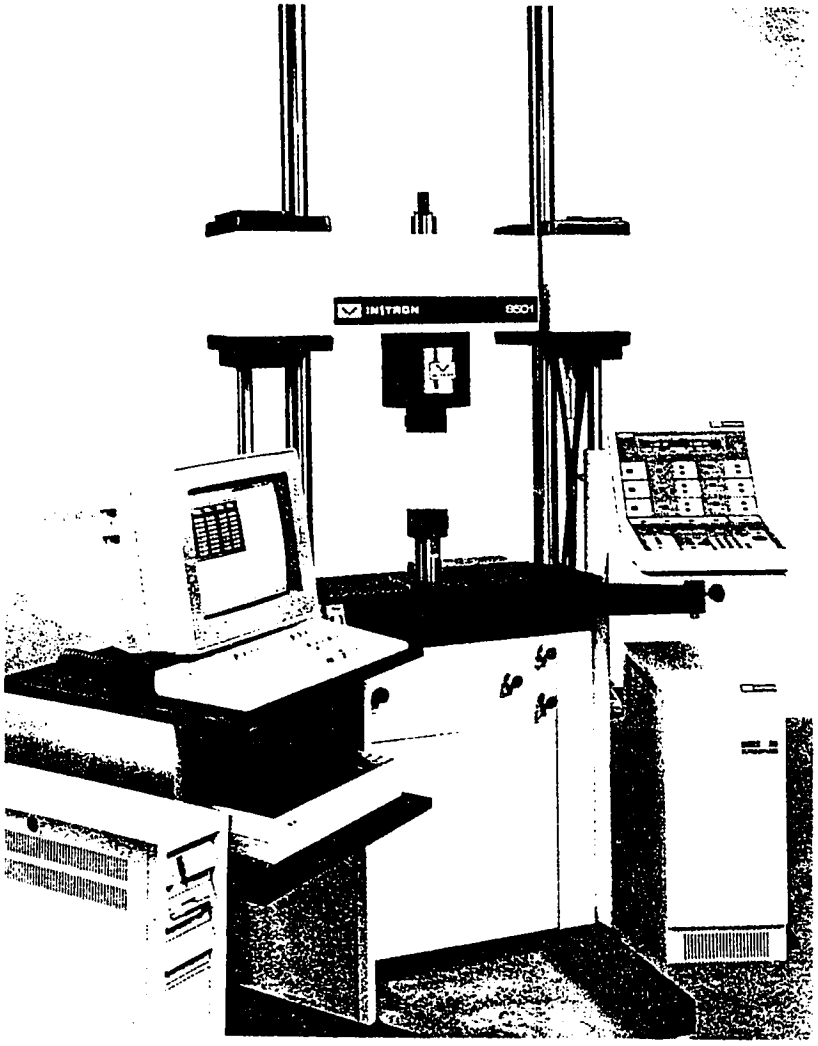

Figure 4.1: Instron 8501 servo hydraulic fatigue testing system.

The resolution of this system was 1.1 microns at 15 cm. The magnification available using eye pieces of 12, 16 and 24 mm were 45X, 35X and 22X respectively. Other combination of more lenses could give higher magnification. The focusing range was between $120mm$ to $400mm$. The microscope was mounted on a table that allowed it to move vertically and horizontally in order to locate the object first, then move along with the crack during propagation to take readings. Pen light focusing arrangement allowed to accurately locate and focus the initial crack instantaneously.

The horizontal mount of the table was hooked up with a horizontal digital recorder with accuracy of measurement up to $0.001mm$. The notch was enlightened by Fostec monochromatic light source with a variable luminosity throughout the tests.

4.1.3 Joel *JSM* T-300

A typical electron microscope produces a small high energy electron spot (beam) by a system of electron-optical lenses to scan across the specimen. The lower energy electrons emitted during scanning are detected, amplified and then used to moderate a recording device cathode ray tube [75]. The electron beam can only be produced in vacuum, so it is done by evacuation of the observation chamber in stages.

Joel JSM T-300 scanning microscope was used to take the fractographs of the fracture surface. The magnification range available was between 1X to 100,000X. The excitation potential was in the range of 1 to 50 KV. Test specimen were reduced to the appropriate size on a shearing machine and mounted on special holders (specially machined for these samples) on the SEM sample holding cross slide in the observation chamber. A general view of the system is given in Fig. (4.2).

To suppress charging and increasing electron emission, gold coating of the fracture surface was also done. This process provides very fine uniform covering of a conducting material (gold), so that the surface coating, is, as nearly as possible, an exact replica of the under lying material, also gold has good electron emission capability in addition to contour accurately on the fractured surface [76]. This coating was done by vacuum deposition in stages provided by rotary and diffusion pumps using a separate instrument. Unfortunately, there was not much difference in the focussing and monitoring of the striations, so, except for the first two samples, other sample were not coated.

4.2 Material and Specimen Geometry

The literature so far surveyed revealed that problem of fatigue is very important for structures and equipment where human lives are at stake e.g. aircrafts, offshore

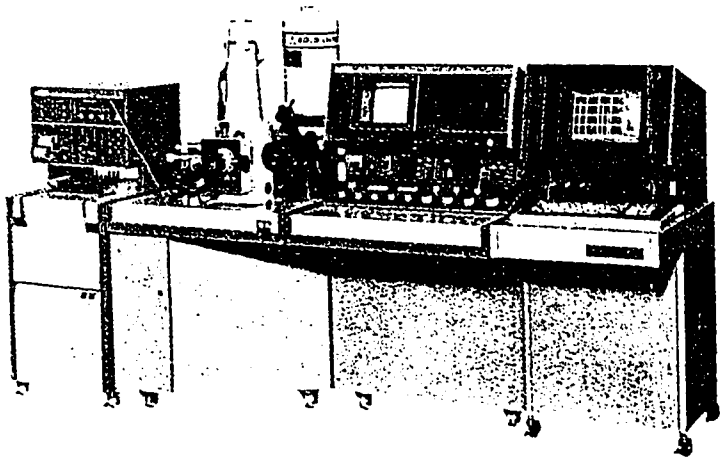

Figure 4.2: The Scanning Electron Microscope, Joel *JSM* T-300.

Specimen	Ni %	Si %	Mn %	Cr %	S %	Cu %
Stainless steel 304l	9.20	0.40	1.70	19.30	0.01	0.20

Table 4.1: Chemical composition.

Specimen	Tensile yield strength	Ultimate tensile strength	elong.
Stainless steel 304	205 MPa	515 MPa	30 %

Table 4.2: Mechanical properties.

structures and platforms, all kinds of bridges, nuclear power plants, pressure vessels etc. The material of interest in these engineering structures are generally high strength steels and aluminum alloys of various grades. But as already stated in chapter 3, that for our investigation we have chosen stainless steel 304 because it is used as structural steel for severe environment which may be subjected to fatigue loading as well.

The blank dimensions were $120 \times 38 \times 1.5mm$, machined parallel to the rolling direction. The notch dimensions are shown in Fig (4.3). The chemical composition and the mechanical properties are given in Table 4.1 and 4.2 respectively. For proper observation of the crack during its propagation life the surface of the sam-

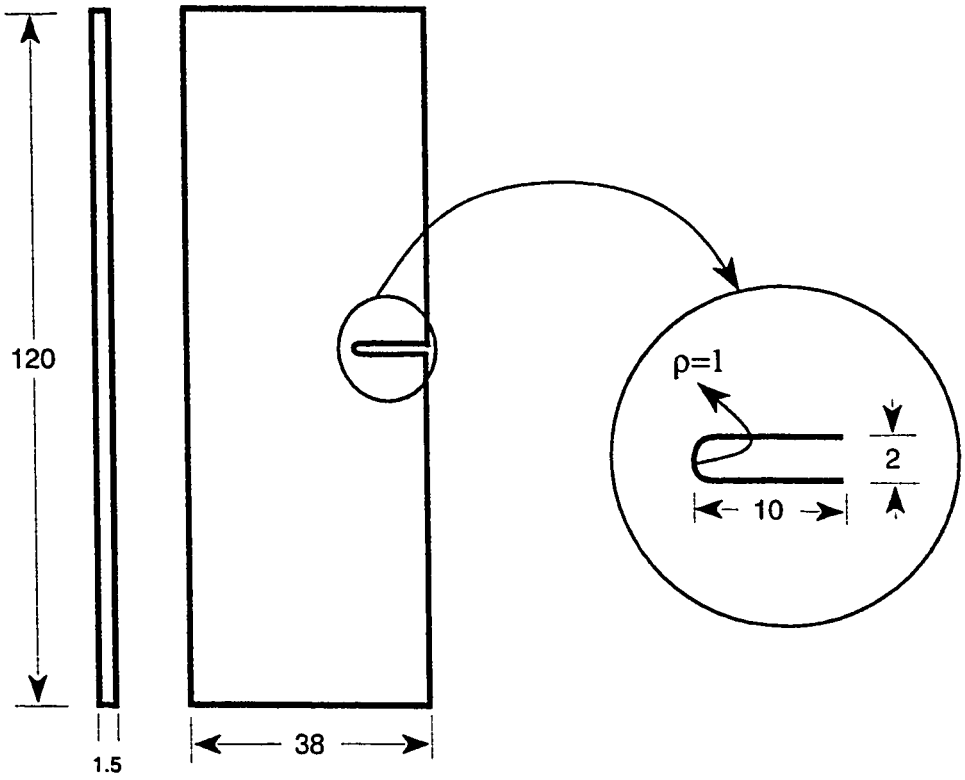

All dimensions in *mm*

Figure 4.3: Geometry of the sample.

ples should be as clean as possible. So, first of all, a physical examination was made for any apparent imperfections in the overall surface and the notch finish. Also, the alignment of the samples was visually checked. Defective samples were rejected. Then, each sample was polished in the vicinity of the crack path using 240, 320, 400 and 600 grit emery papers, perpendicular and then parallel to the crack direction in a sequence that would end in 600 grit emery, applying last in perpendicular to the crack direction.

After each fatigue test, the fractured samples were stored in the decicator to protect the fracture surface from any atmospheric contamination. Later, the fracture surface was first ultrasonically cleaned in acetone for three to four minutes and dried by blowing air to the samples before SEM analysis.

4.3 Design and Generation of VAL Histories

The fatigue life is estimated for different VAL loading conditions. These conditions were generated using elemental sinusoidal waveform for all cases. The R ratio for all VAL tests was maintained as $\frac{1}{7}$. For the generation of these loads special instructions were written using FLAPS software. The details of these histories are described as under:

4.3.1 Single Tensile OL

For stainless steel samples, all tests were composed of two tasks per block. First: the constant amplitude part running for n number of cycles at $10Hz$, second; the OL part at $0.1Hz$ which was one half of a sine cycle (except for sample # 9). These blocks were repeated to generate the VAL loading history at $10Hz$. (P_{mean}) was 4 KN and amplitude $\pm 3KN$ (giving ΔD P as 6KN. P_{max} as 7 KN and P_{min} as 1 KN. The number of cycles (n) in the CA part, ranged from 5000, 1000 and 100, with the peak (OL) at 9 KN for sample numbers 4, 5 and 6 respectively (see Fig. 4.4(a)). To observe the effect of the magnitude of OL, the OL was raised to 11 KN and 13 KN for sample numbers 10 and 11, respectively.

4.3.2 Multiple OL's

Replacing the OL part from the block of single OL (4.3.1, just described) with 5 successive OLs, thereby generating multiple OLs. The details of the block are given in Fig, 4.4 (b). This block was then repeated to form the VAL history using FLAPS.

4.3.3 CAL

For comparing the VAL data two CAL loading under similar conditions (i.e. ΔP $= 6KN$) were also run for sample numbers 13 and 15 with mean load 4 KN ($\pm 3KN$). Jones [53] had also reproduced two CAL test to give confidance in his base reference

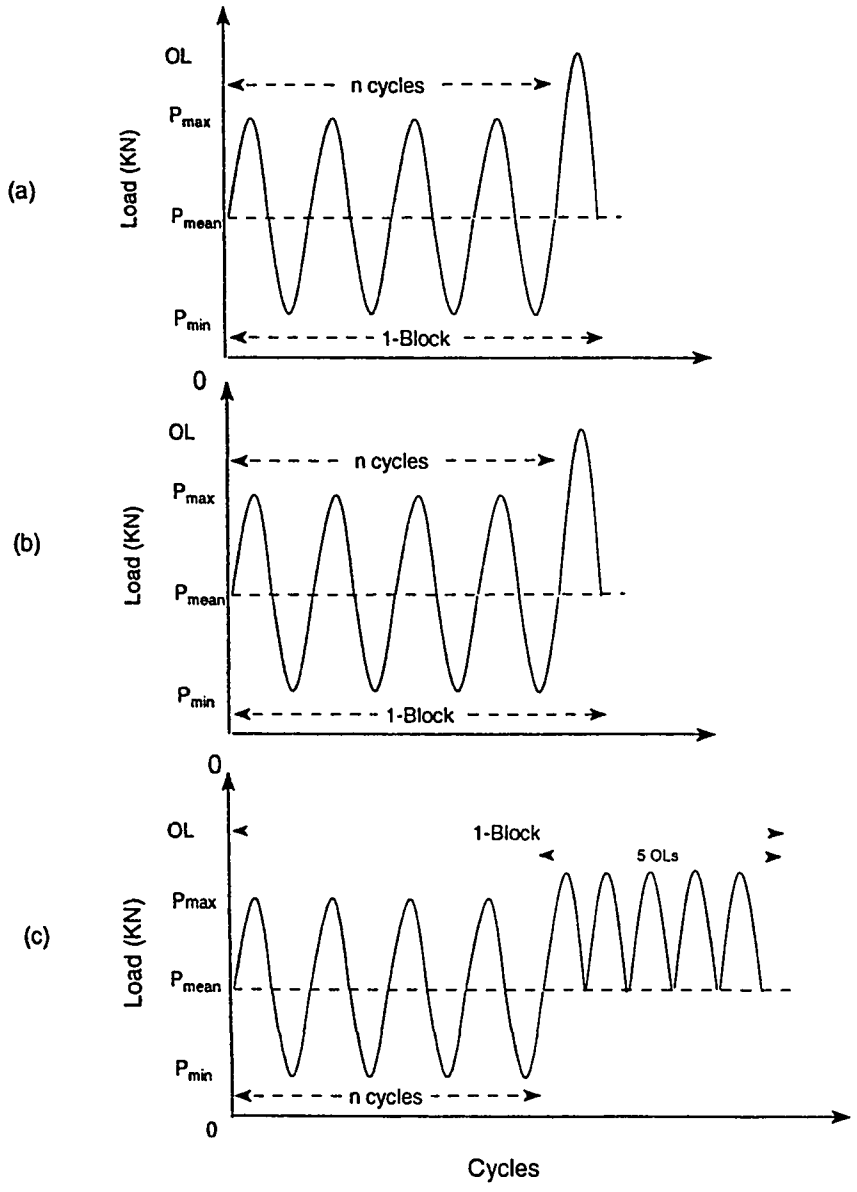

Figure 4.4: VAL loading histories. (a) OL=9KN, $n = 5000, 1000, 100$ (b) n=1000, OL=9KN, 11KN, 13KN (c) multiple OL's 5, $n = 1000$ with $P_{mean} = 4 \pm 3KN$

CAL test. The results of both these tests were quite identical which also showed the reproducibility of our system. So, their combined representation (S # 135) is taken as the reference CAL.

4.4 Collection of Data

For our investigation, the pre-cracking was done at room temperature at high loads $5 \pm 3.5KN$ in magnitude and $10Hz$ in frequency . The horizontally travelling microscope was placed in front of Instron 8501 at a distance of about $200mm$, on a platform that shielded it from the vibrations of Instron 8501. Before starting each test, the the notch was focused and then CAL was applied for pre-cracking.

The notch was then continuously observed for appearance of any crack using $16mm$ lense. Once detected, the crack was monitored till it approached $0.001m$ mark. This crack length is assumed to be well beyond the crack initiation length and crack is believed to be in the propagation stage of its life. That crack length was also the initial crack length for FCP. The CAL was discontinued at that point recording the initial crack length a_i and the corresponding cycles N.

In the beginning, *Loop Shaping* of the system was done. This is recommended whenever a new test sample with new dimensions is tested on Instron system through

FLAPS. The signal input from the computer is adjusted according to the Instron's actuators's response using an oscilloscope by adjusting the P.D.I values (Proportional, Derivative and Integrator gains). Once set, these values are retained in a separate file for that particular geometry.

VAL was then applied using a $486DX$ microprocessor interfaced with Instron 8501 system through GPIB card. From then on, crack lengths and corresponding cycles were recorded intermittently using the Questar microscope horizontal control and the Instron control panel respectively, till final failure. The collection of data was slack at the beginning, steady at the middle and rapid at the end of the fatigue process. Some still photographs were also captured during the tests using another $16mm$ lense. The crack growth from the notch and its propagation as collected from a $16mm$ Questar lense mounted on a still camera on the axial opening. Views of how a crack grows are shown in Figs. (4.5) and (4.6).

4.5 Examination of The Fracture Surface

The fractured samples were held in the sample holder vertically and slided over the cross slide of the specimen chamber of the SEM. The chamber was then evacuated. The excitation potential or the beam voltage was kept at 20 KV. For our analysis, magnification used was in the range of 50X (for initial positioning) upto 7500X

for detection and capturing the possible sites. The fracture surface was focused at different magnifications and then scanned along a direction perpendicular to the advancing crack, from one edge to the other, successively from the fractured end to the notched end for possible striation sites.

The sites for locating striations had to be very carefully chosen for best details and resolution. To ease locating the desired sites, comparatively flat areas are scanned using low magnification (200 to 750 X). Such sites are observed at different magnifications to locate signs of striations. With no such details caught, new site is scanned at low magnification again. For each fractograph the position from the notch was initially recorded as datum on the micrometer (mounted on the cross slide, provided on the side of the observation chamber). The fractographs were exposed at the shutter speed of 1/60 *sec.*

The striation spacing, magnification, number of striations per unit distance on the fractograph were used to calculate the FCP rate using equation (3.12). Few fractographs are shown in Figs. (4.7) and (4.8).

Now, with the basic fatigue data in hand we are in a position to use it and obtain the parameters required for analysis.

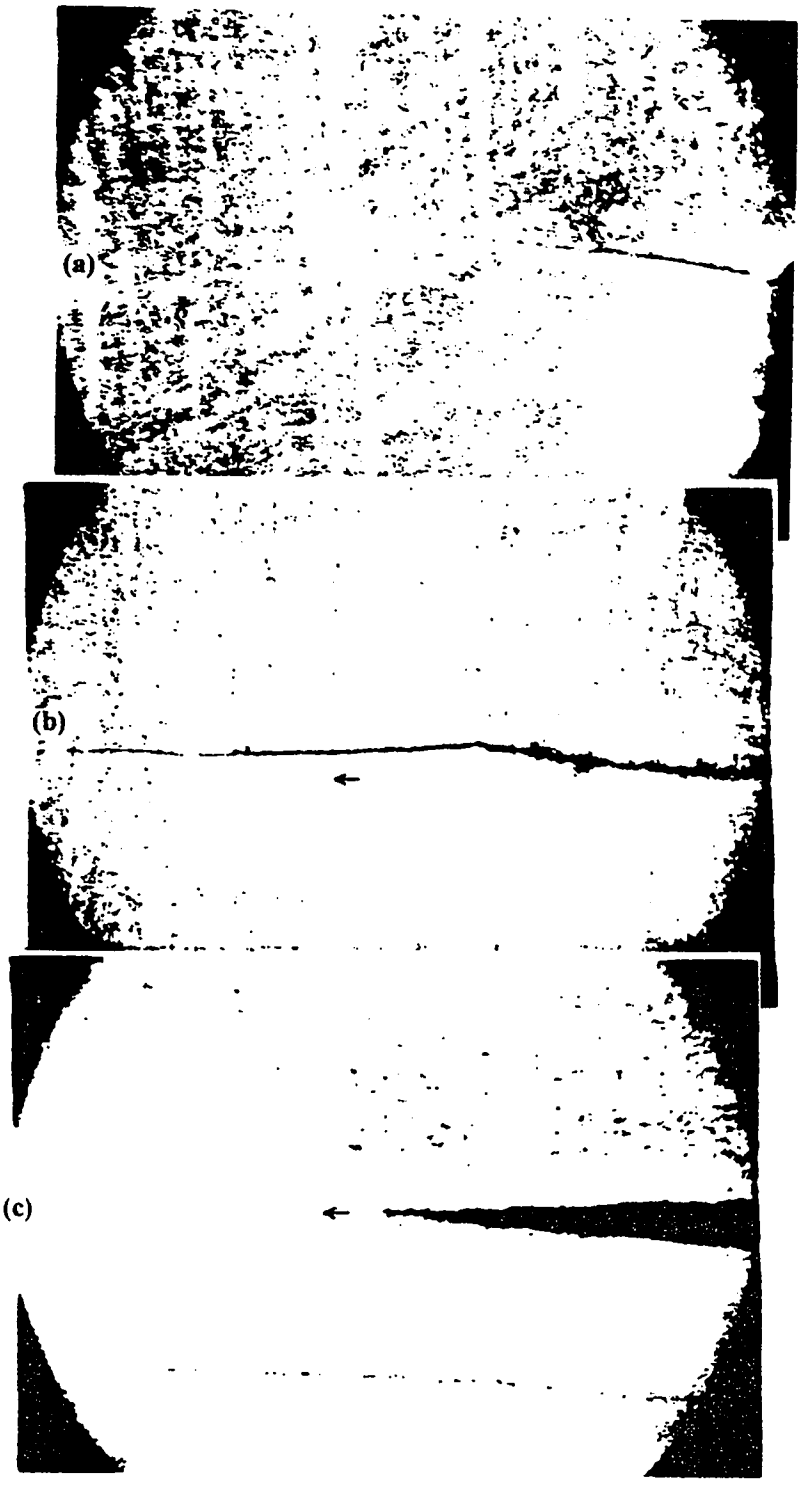

Figure 4.5: (a) crack at pre-cracking, (b) and (c) at various stages.

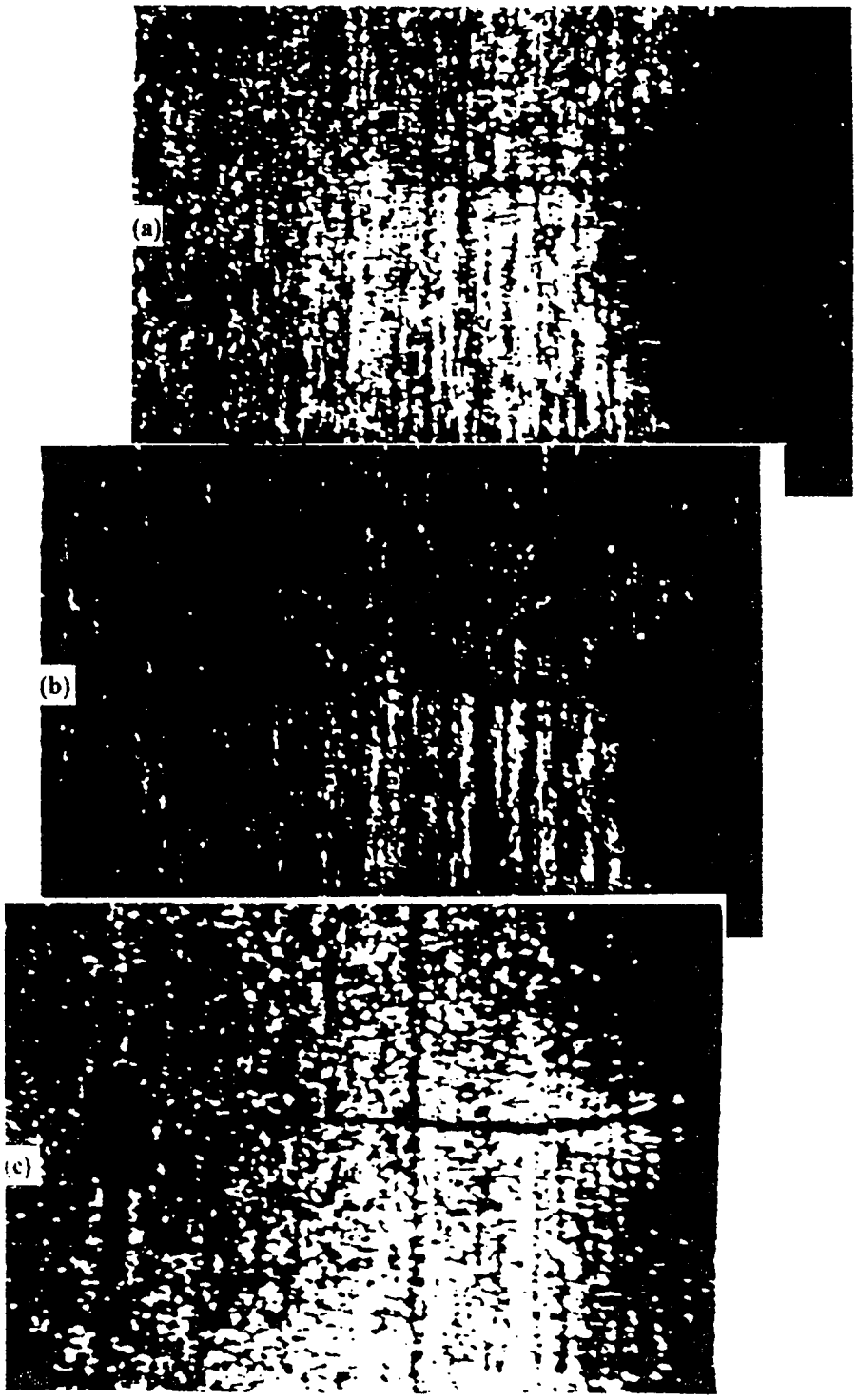

Figure 4.6: (a) crack at pre-cracking, (b) and (c) at various stages.

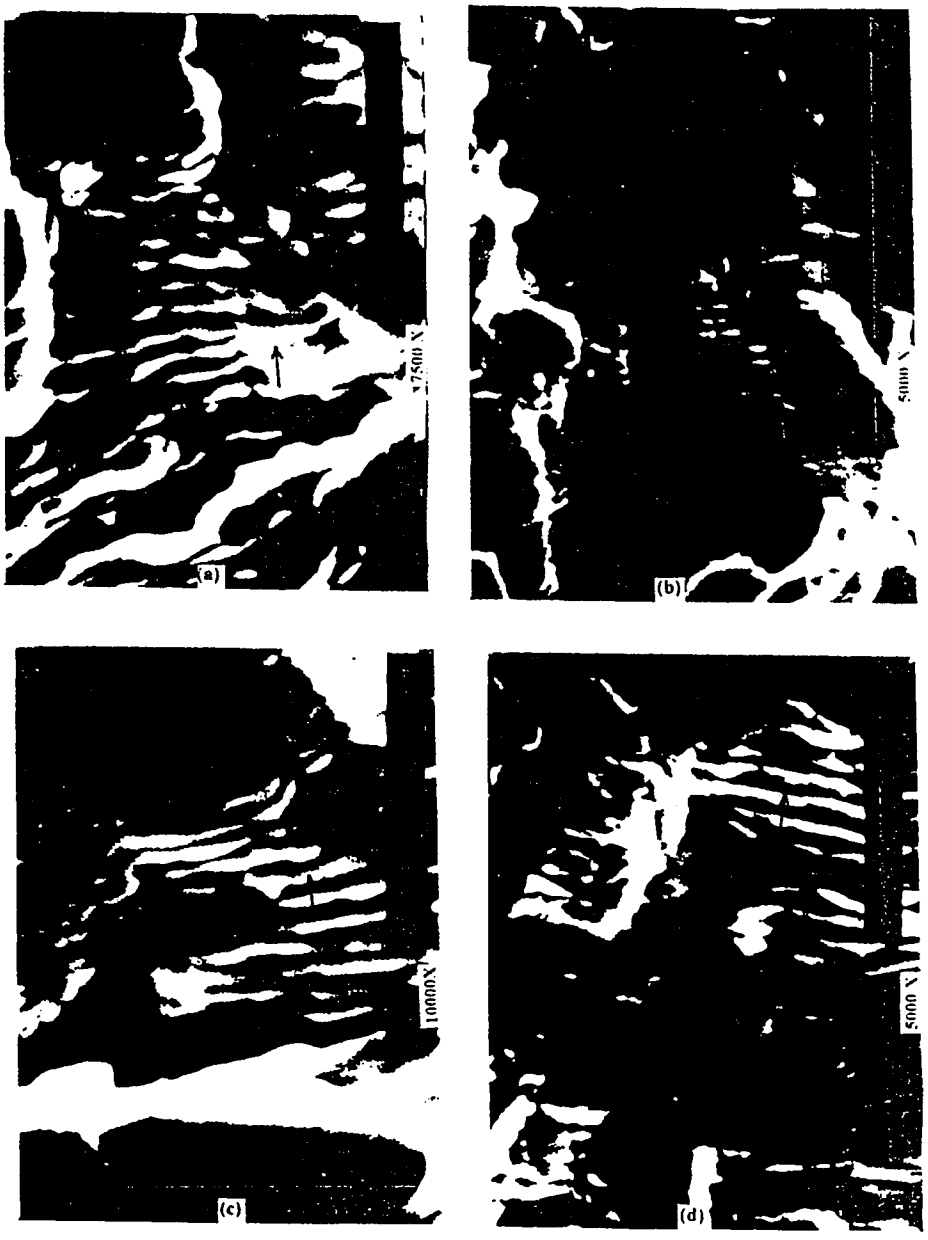

Figure 4.7: Fractographs showing fatigue striations at different magnifications.

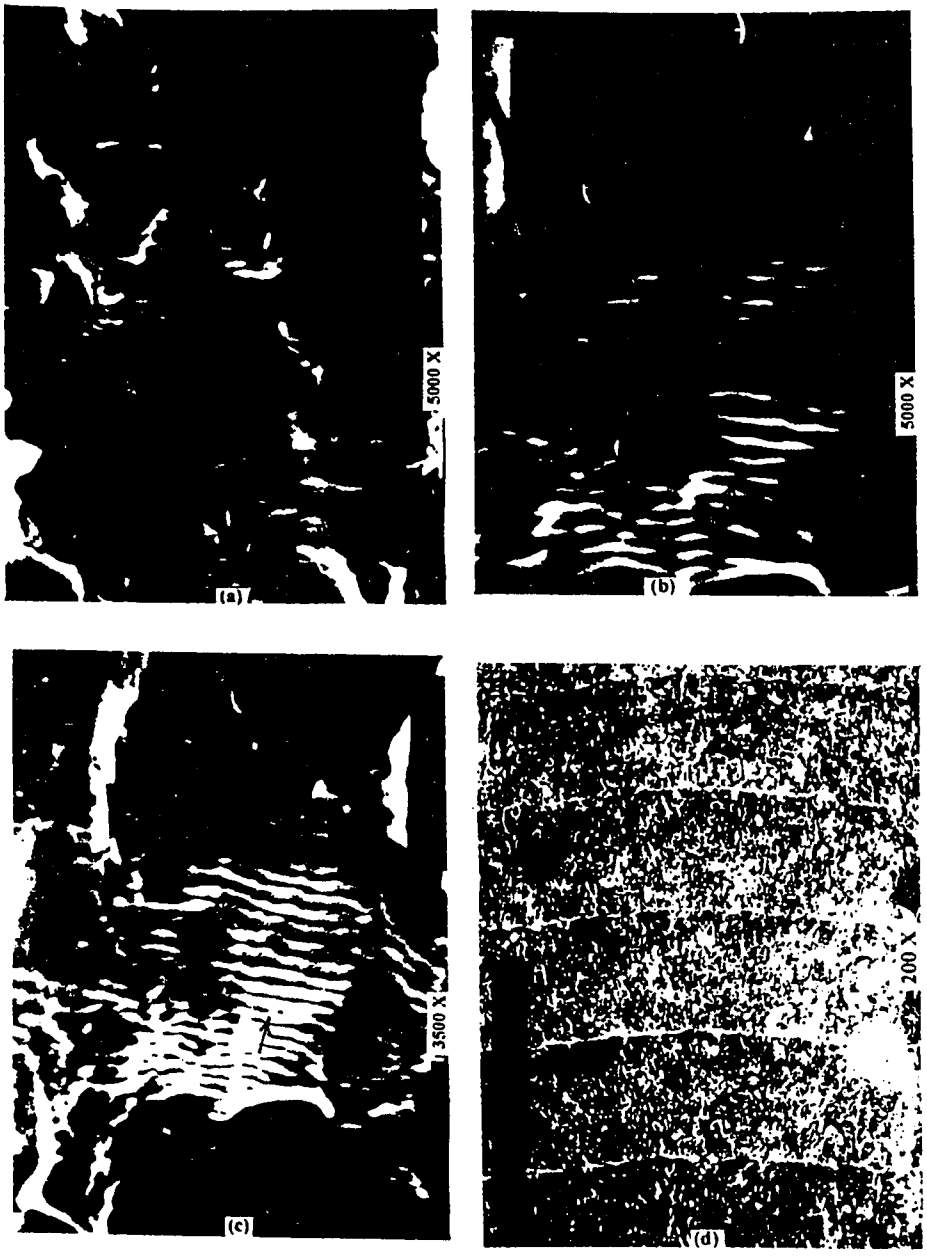

Figure 4.8: (a), (b) and (c): Fractographs showing fatigue striations. (d) Crack arrest marks.

Chapter 5

Computation of Results

5.1 Calculation of FCG Rates

For determining FCG rates a Vs N data is plotted on a linear paper shown in Fig. (5.1). The crack growth trend is also shown this figure . Slopes $\frac{da}{dN}$ were calculated from each a Vs N curve. ΔK was calculated from equation (3.2). For each case $\frac{da}{dN}$ and ΔK was used to calculate the Paris constants i.e slope (m) and the y-intercept (C), by linear regression on a log-log paper.

Direct calculations technique, taking successive slopes at each data point on the a Vs N curve was also used by Pook [73]. Same method has been used here to calculate the C and m values. The FCG rate curves thus obtained are shown in Figs. (5.2 to 5.11).

The literature shows that the value of m for steels lie within the range of $2 < m < 4$ [20, 73], and $2 < m < 5$ [77]. Table 5.1 shows the values of m and C obtained by calculations and these are within these ranges.

Sample Nos.	m	C (m/cycles)
4	3.386	1.26×10^{-12}
5	4.32	7.52×10^{-14}
6	3.64	7.033×10^{-13}
9	3.126	8.71×10^{-12}
10	3.744	8.34×10^{-13}
11	2.58	3.306×10^{-11}
12	2.899	7.71×10^{-12}
13 CA	2.45	1.18×10^{-10}
15 CA	3.454	4.83×10^{-12}
135 CA	3.458	1.339×10^{-11}

Table 5.1: Paris constants m and C.

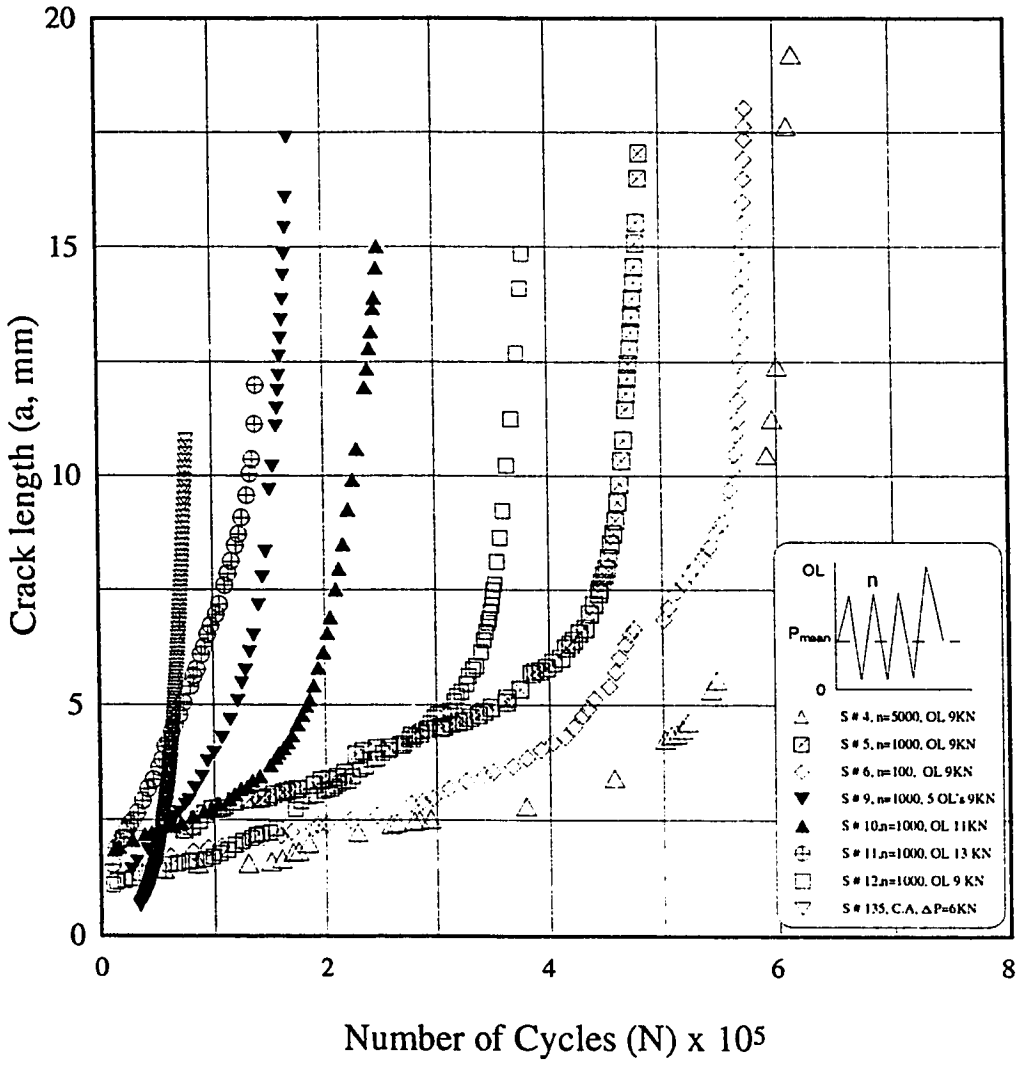

Figure 5.1: a Vs N for stainless steel 304 under different VAL conditions.

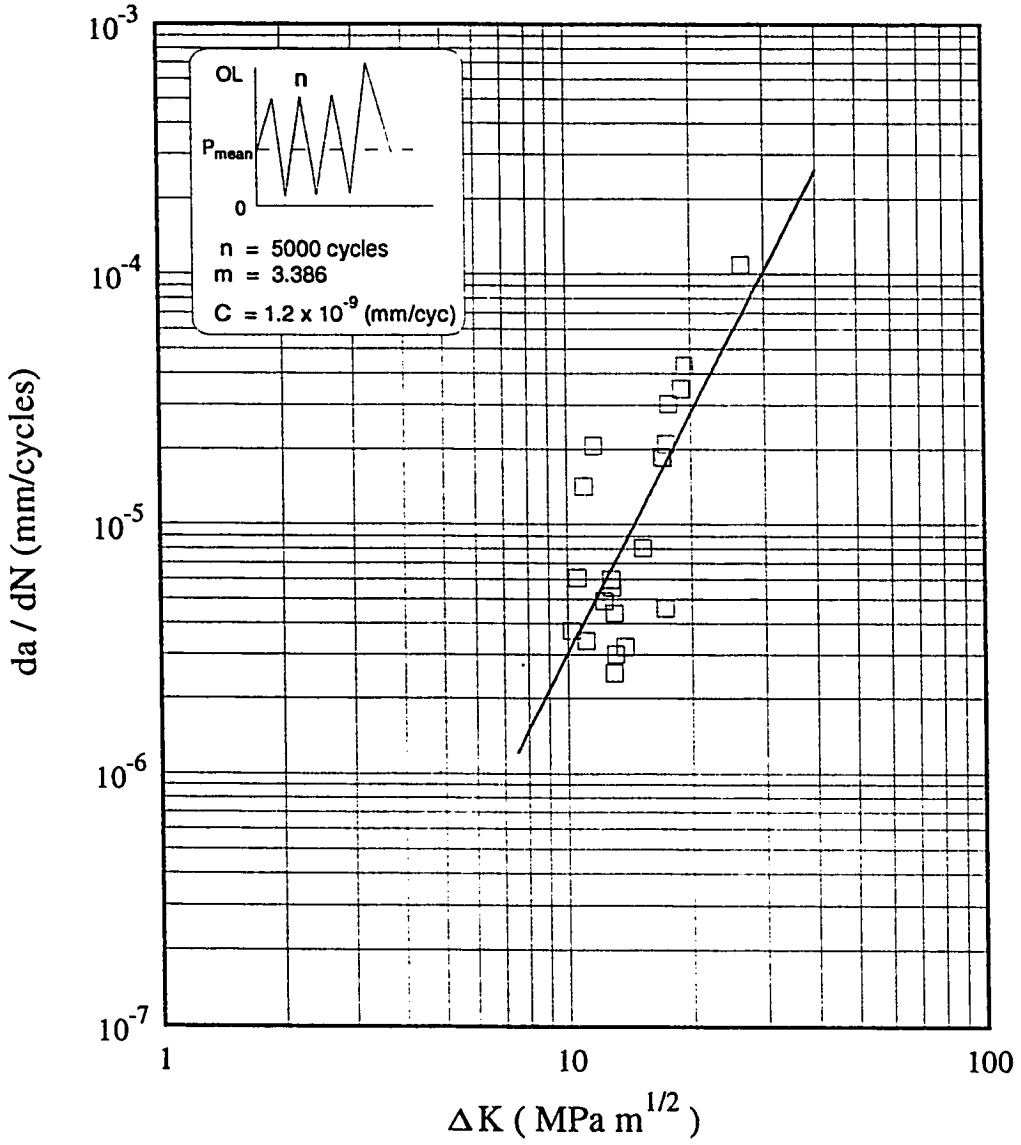

Figure 5.2: FCG rate versus stress intensity factor range, specimen tested with base CAL cycles at n=5000, 10 Hz and single OL at 9KN.

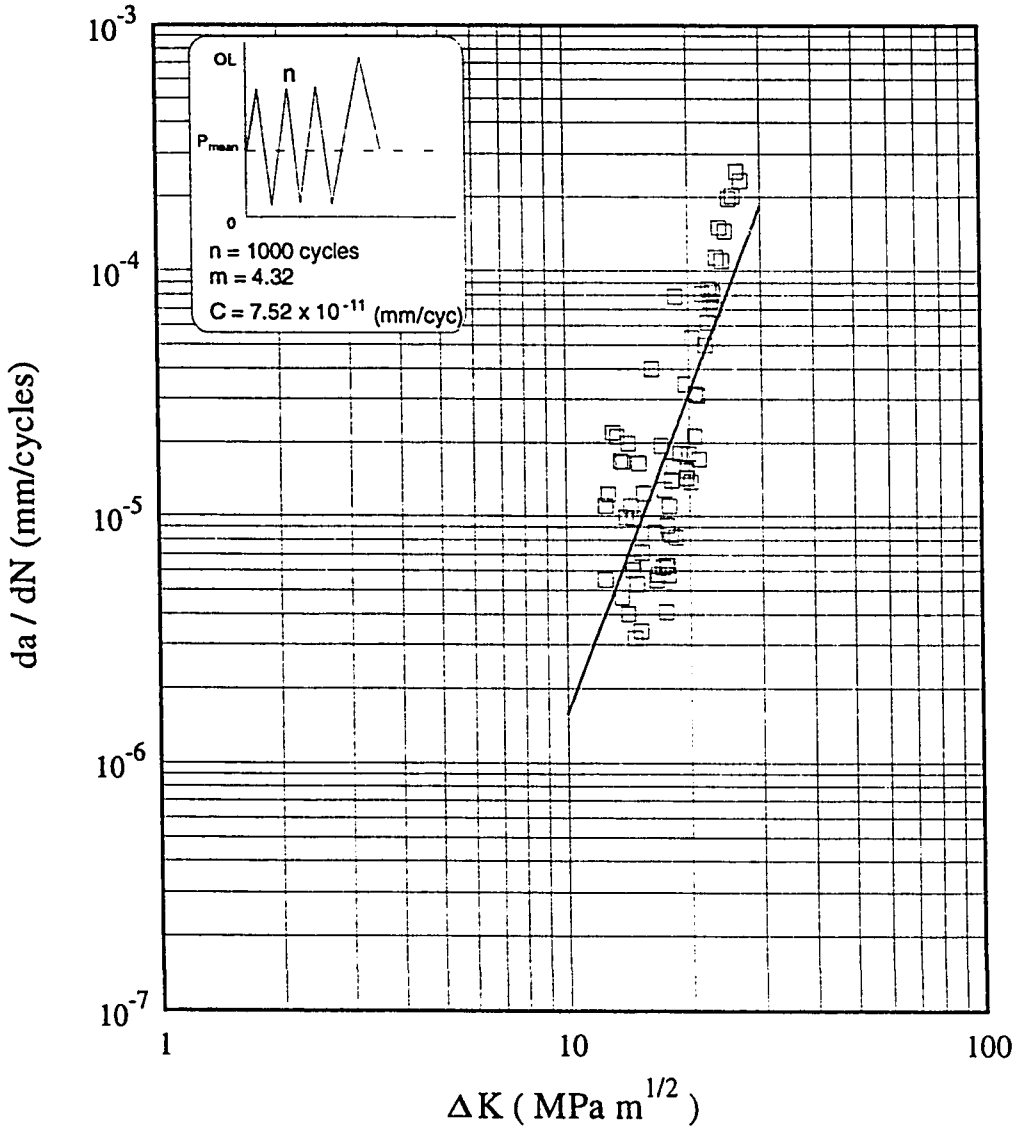

Figure 5.3: FCG rate versus stress intensity factor range, specimen tested with base CAL cycles at n=1000, 10 Hz and single OL at 9KN.

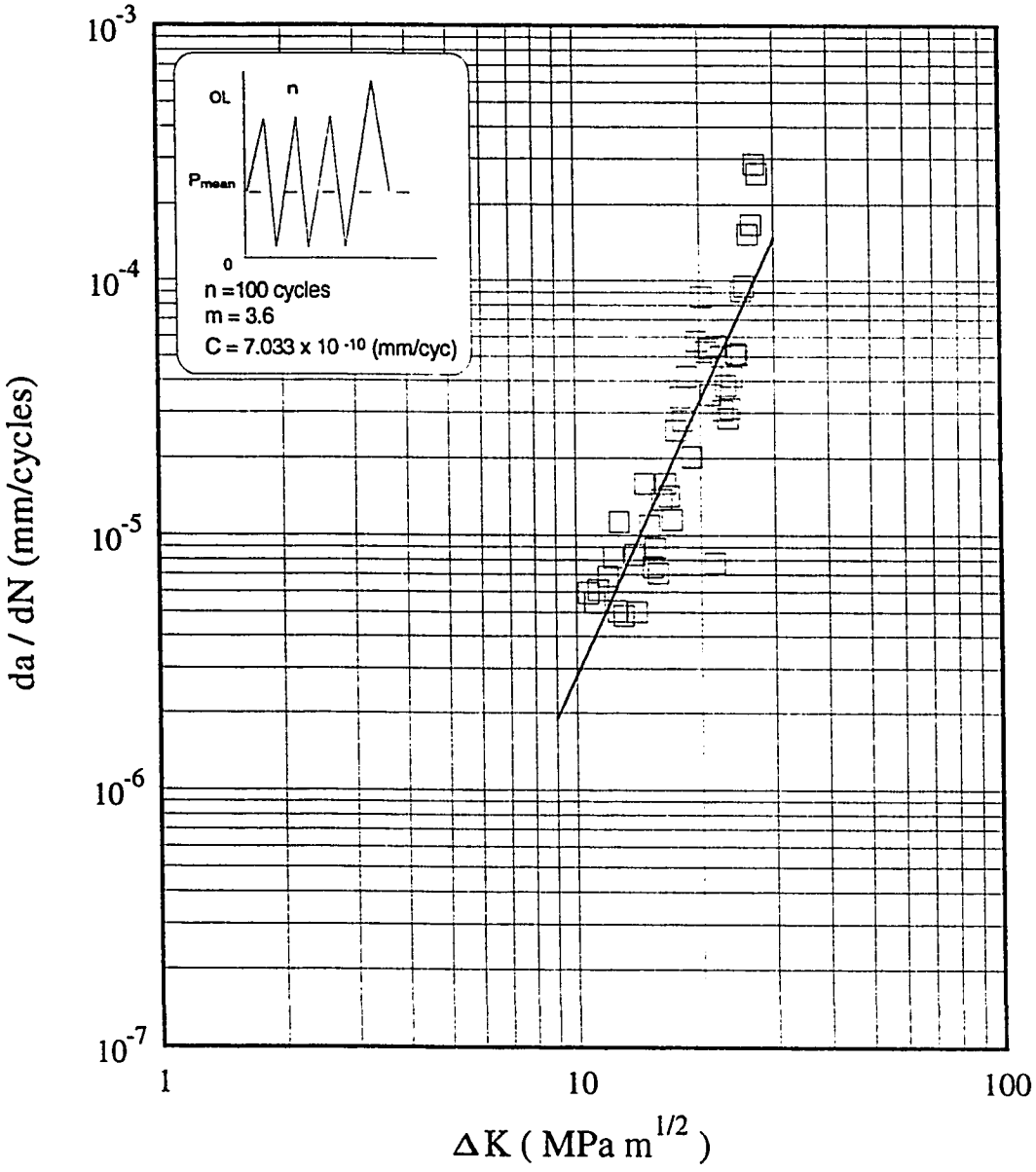

Figure 5.4: FCG rate versus stress intensity factor range, specimen tested with base CAL cycles at n=100, 10 Hz and single OL at 9KN.

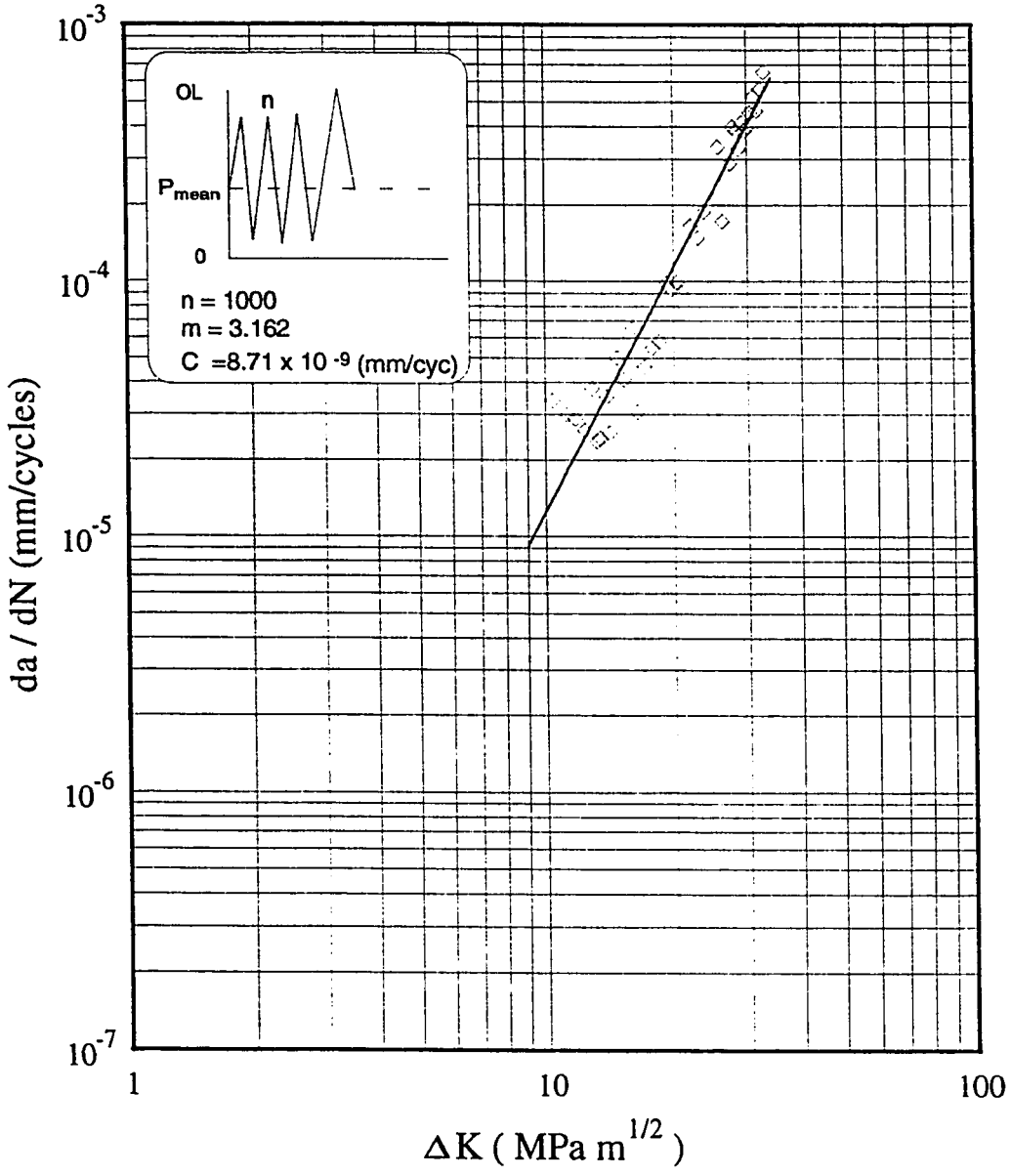

Figure 5.5: FCG rate versus stress intensity factor range, specimen tested with base CAL cycles at n=1000, 10 Hz and five OL at 9KN.

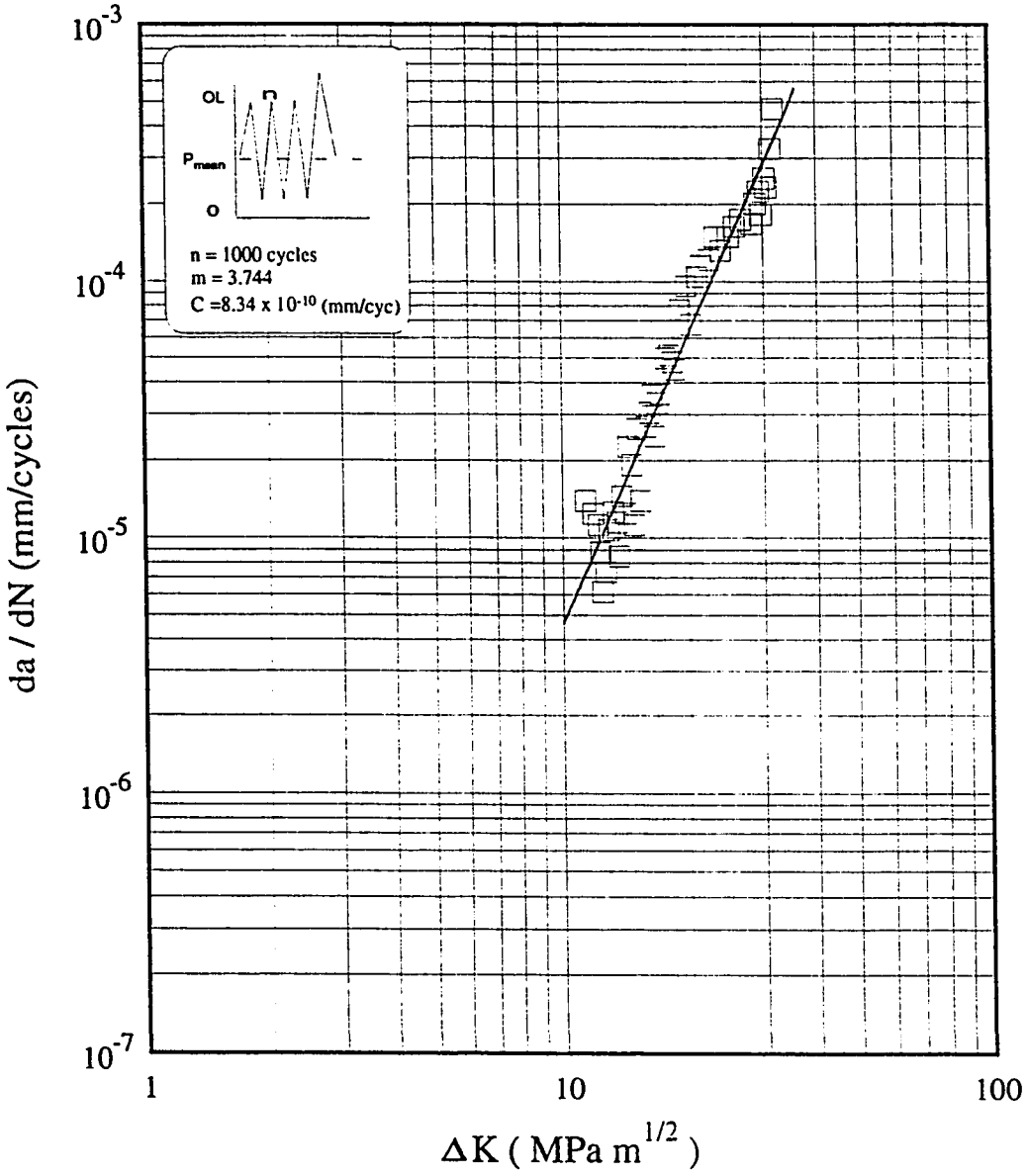

Figure 5.6: FCG rate versus stress intensity factor range, specimen tested with base CAL cycles at n=1000, 10 Hz and single OL at 11KN.

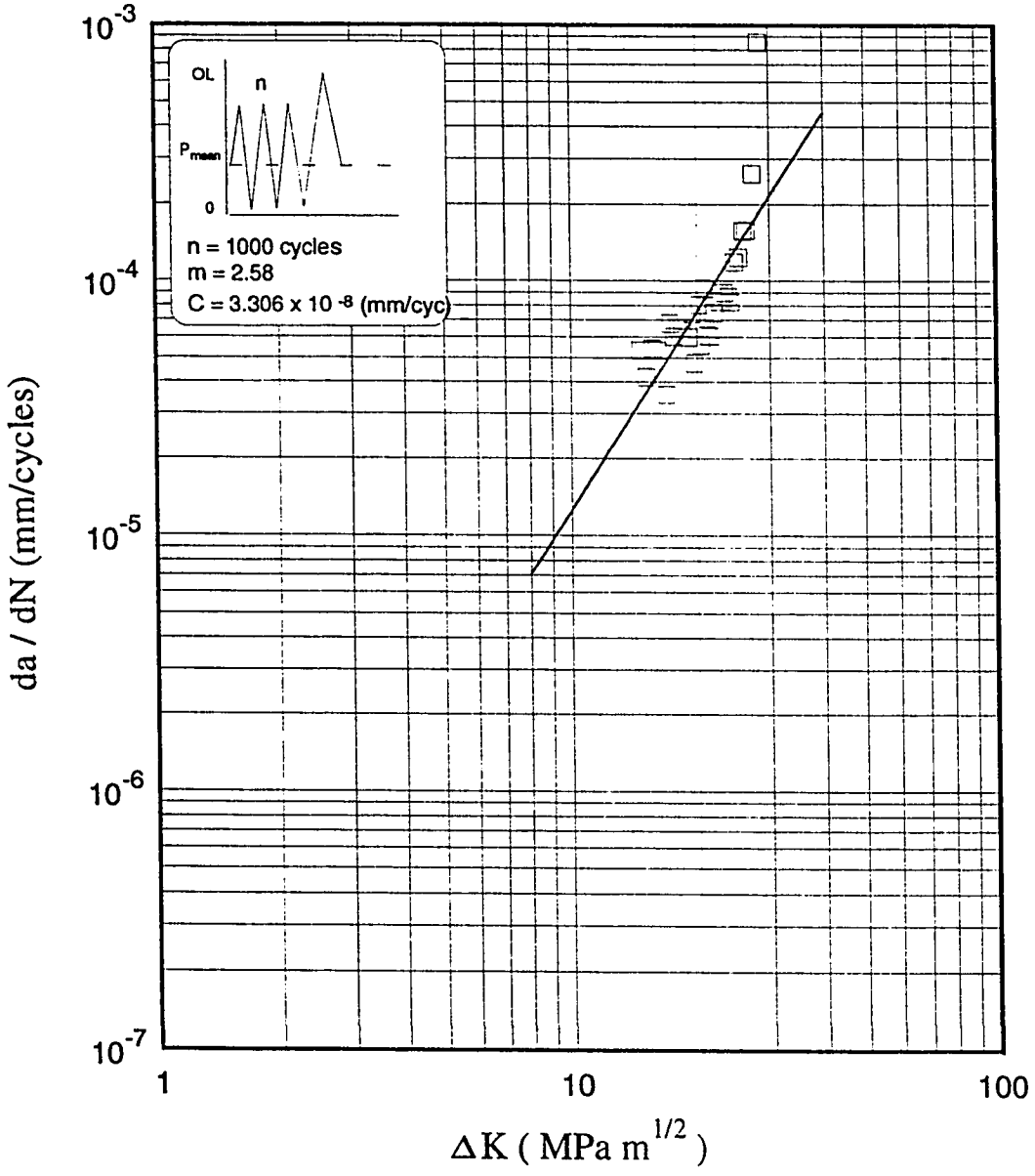

Figure 5.7: FCG rate versus stress intensity factor range, specimen tested with base CAL cycles at n=5000, 10 Hz and single OL at 13KN.

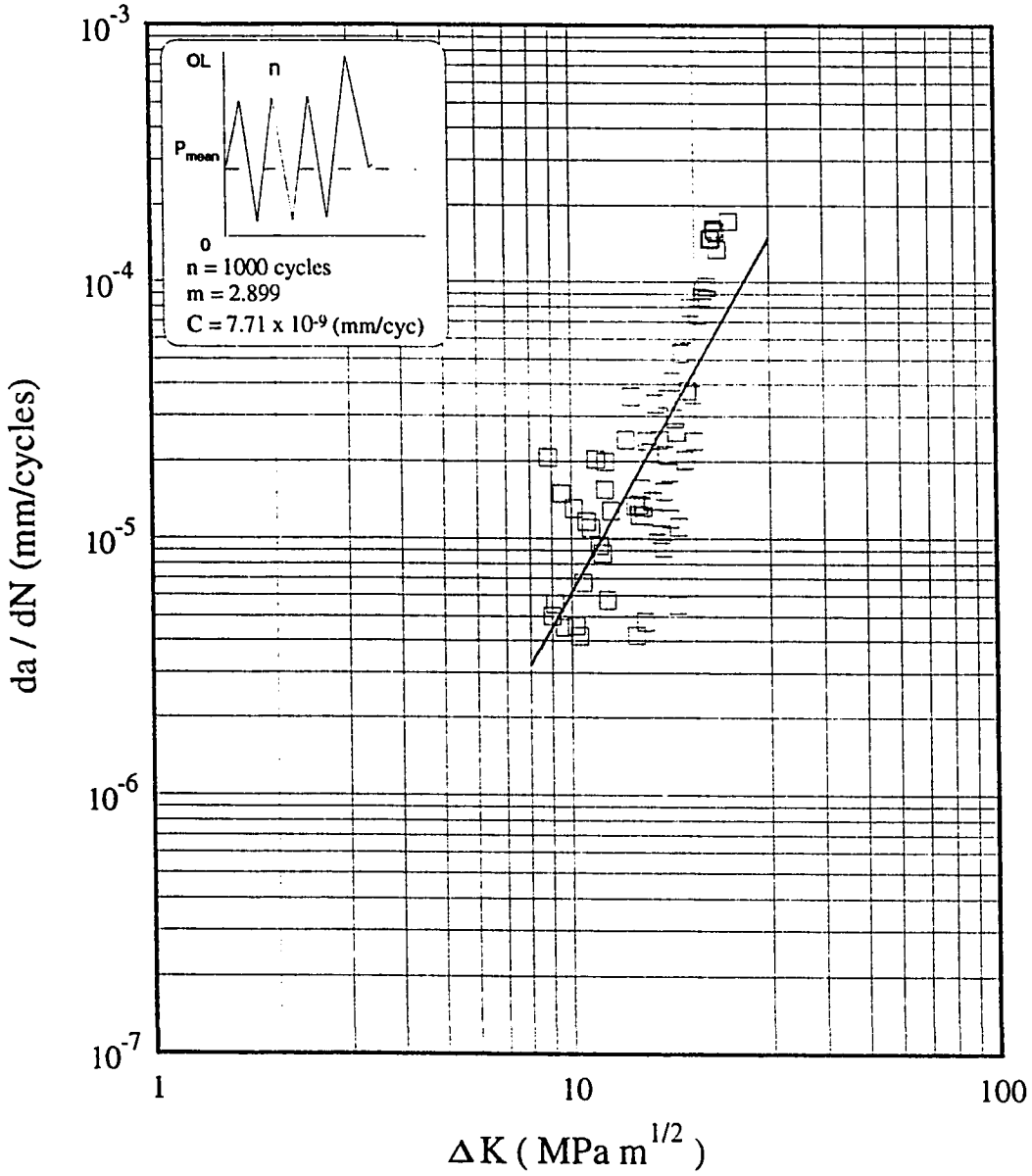

Figure 5.8: FCG rate versus stress intensity factor range, specimen tested with base CAL cycles at n=1000, 10 Hz and single OL at 9KN.

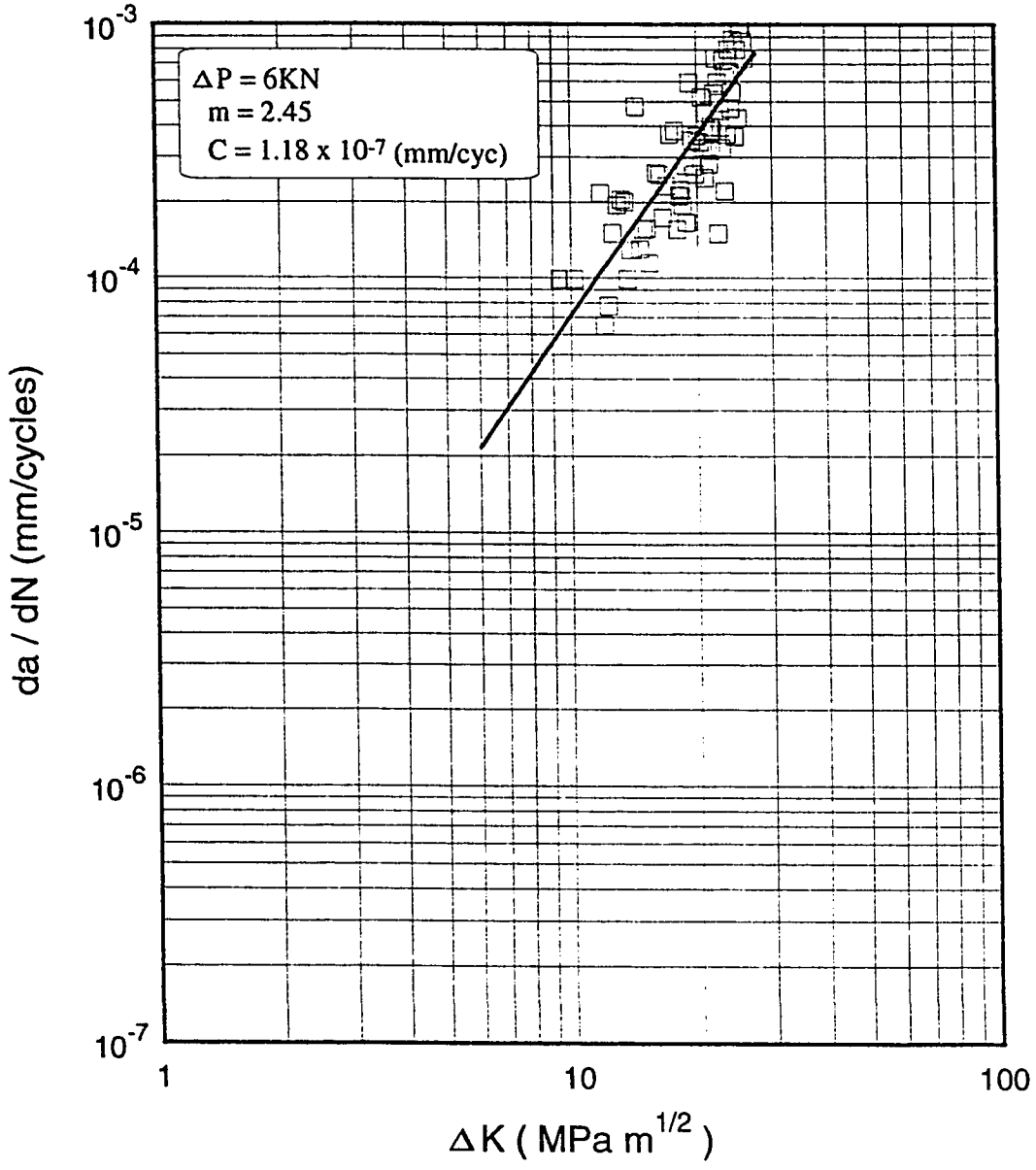

Figure 5.9: FCG rate versus stress intensity factor range, first specimen (# 13) tested at CAL with $\Delta P = 6KN$ at 10 Hz.

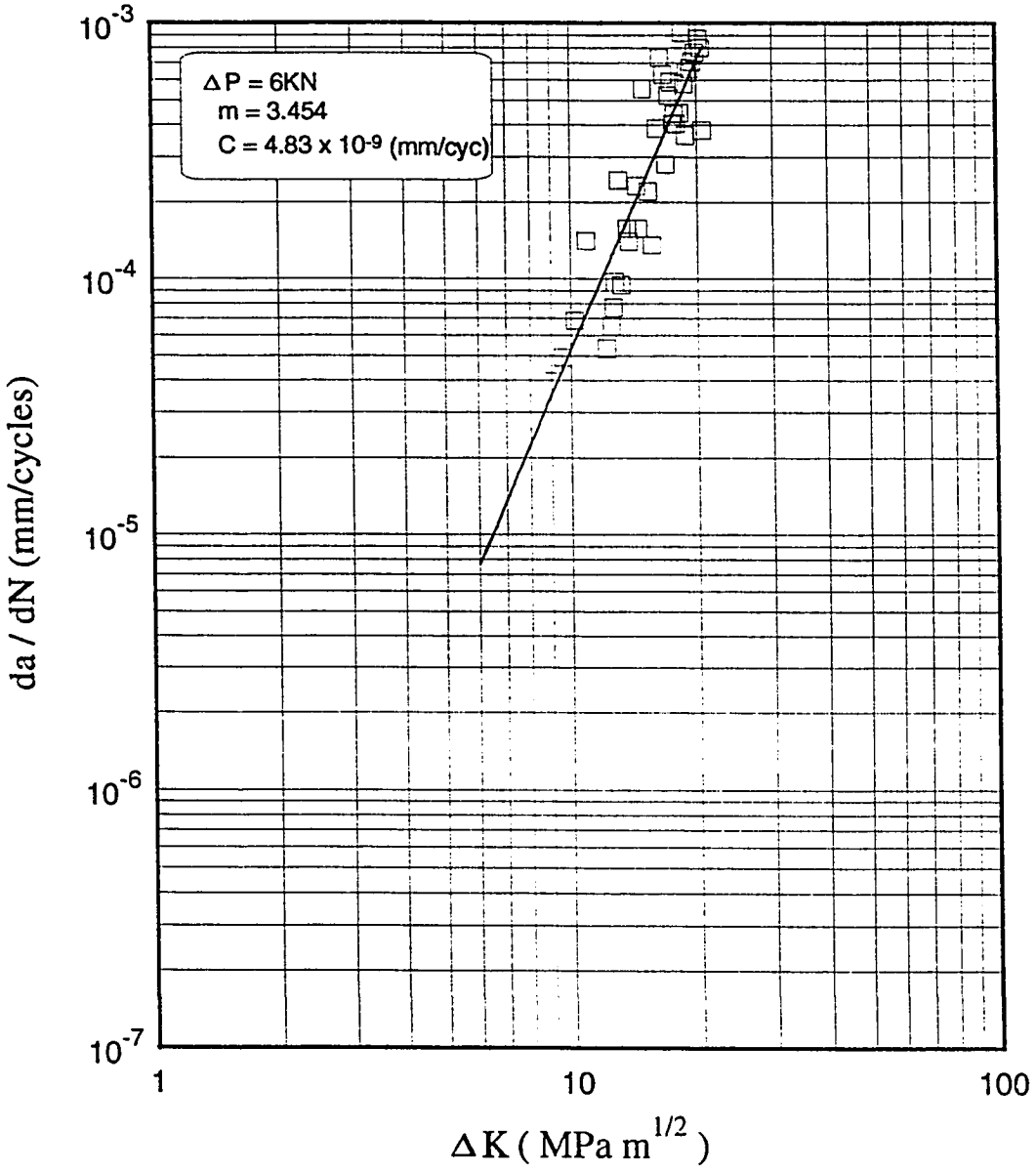

Figure 5.10: FCG rate versus stress intensity factor range, second specimen (# 15) tested at CAL with $\Delta P = 6KN$ at 10 Hz.

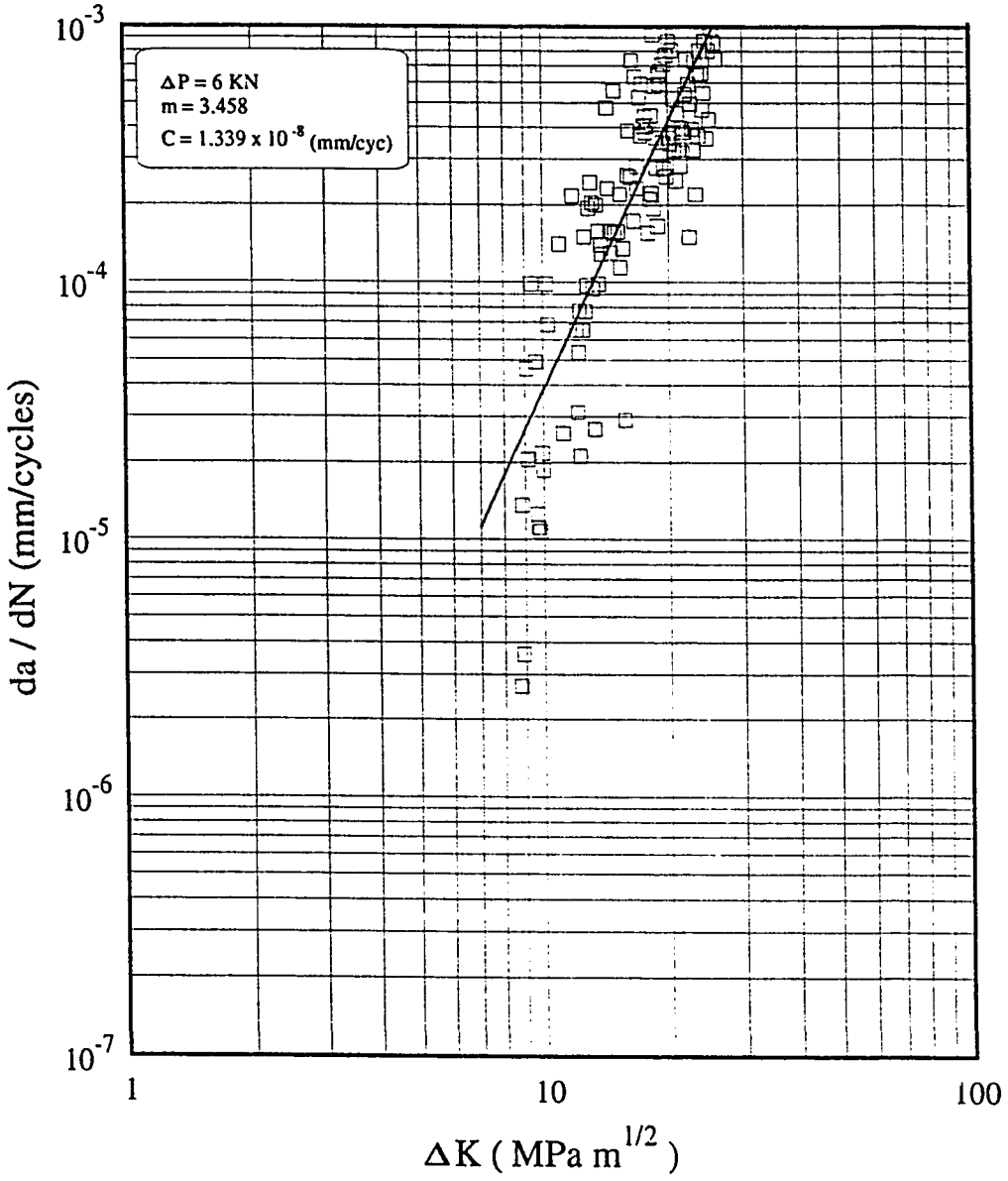

Figure 5.11: FCG rate versus stress intensity factor range, specimen 13 and 15 combined

5.2 Fatigue Life Prediction

The usual scatter in the experimental fatigue data could range from 2*to*4. In general practice, a model is considered to be reasonably accurate and reliable if the ratio of predicted to experimental fatigue life lie within the range of 0.5 to 2 i.e within a factor of two [78]. A model giving fatigue life within a factor of three range is also considered acceptable. Some researchers have also reported their results within a factor of 5, [79]. It is interesting to note that on one occasion 235 samples were tested under similar conditions and gave fatigue lives in the range of 1×10^4 to 10×10^4.

5.2.1 Wheeler's Model

Paris Equation

Using equation (3.5), the FCP lives were obtained by integration of the Wheeler's model using Paris equation for each sample. These results along with their corresponding experimental results are shown in Fig. (5.12). The shaping parameter p for steel had been taken as 1.2, the geometric factor $f(g)$ as 1.12 [48, 71], a_i as per the experimental reading (around 0.001 mm), a_f from equation 3.6. Different loads used are given in chapter 4 (section 4.3), and the dimensions in Fig. (4.3).

Modified Paris Equation (with R ratio)

The modified paris equation (3.8) was used for calculating the FCP lives of each sample. These results of FCP lives are presented graphically in Fig. (5.13).

5.2.2 Elber's Model

Using equation (3.2) in equation (3.11) then integrating gave the fatigue lives as predicted by the Elber's model. These results are also plotted against the experimental data in Fig. (5.14).

5.2.3 Fractographic Approach

For obtaining FCG rates through fractography, equation (3.12) was used. The number of striations and their separation (in mm) were counted on each fractograph which gave the FCG rates for that particular sample at a particular crack length. Unfortunately, the striations were not easily visible on all the samples. Only samples numbered 5, 6, 9 and 10 revealed some striations, if any. These striations were localized in the final crack development regions. Some of these fractographs have been shown in chapter 4.

The analysis of these results is presented in the following chapter.

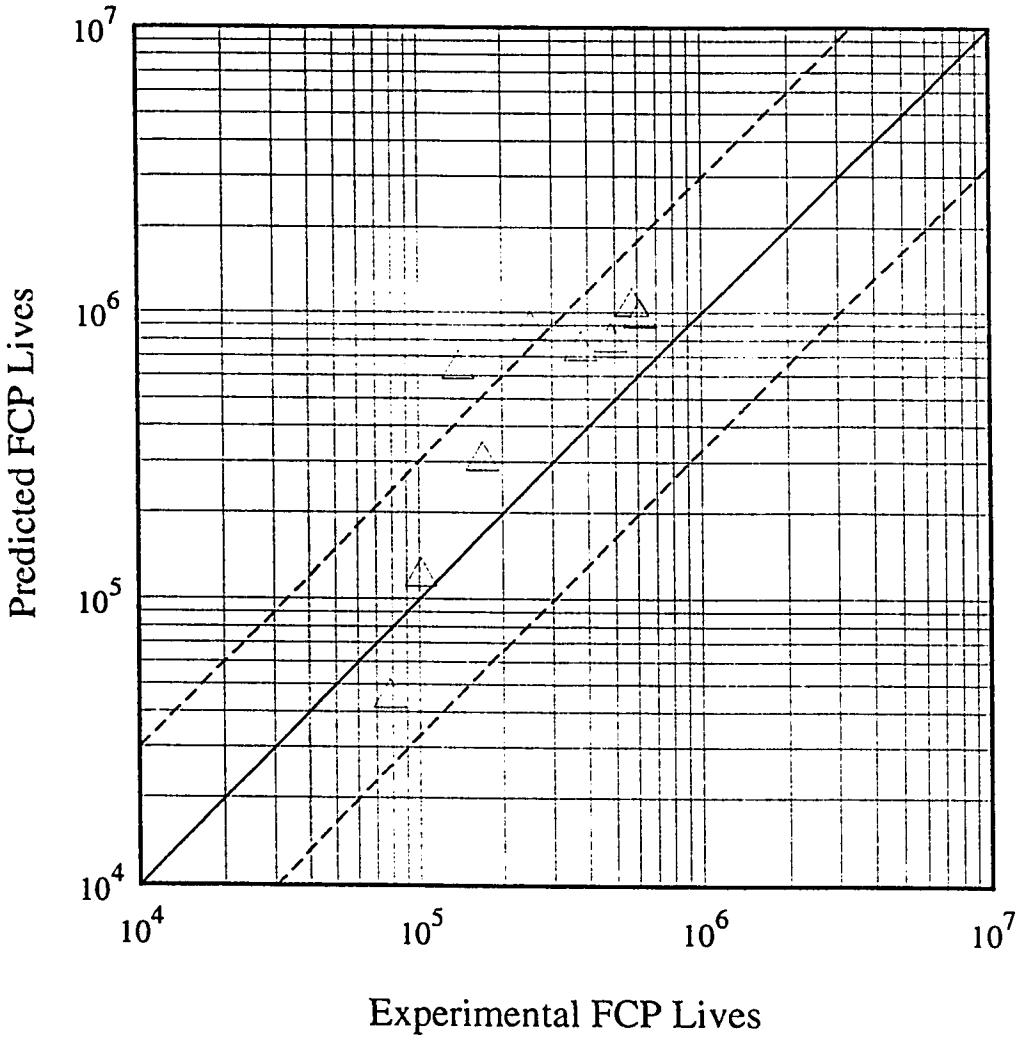

Figure 5.12: Fatigue Lives; Experimental Vs Wheeler's prediction (using Paris equation).

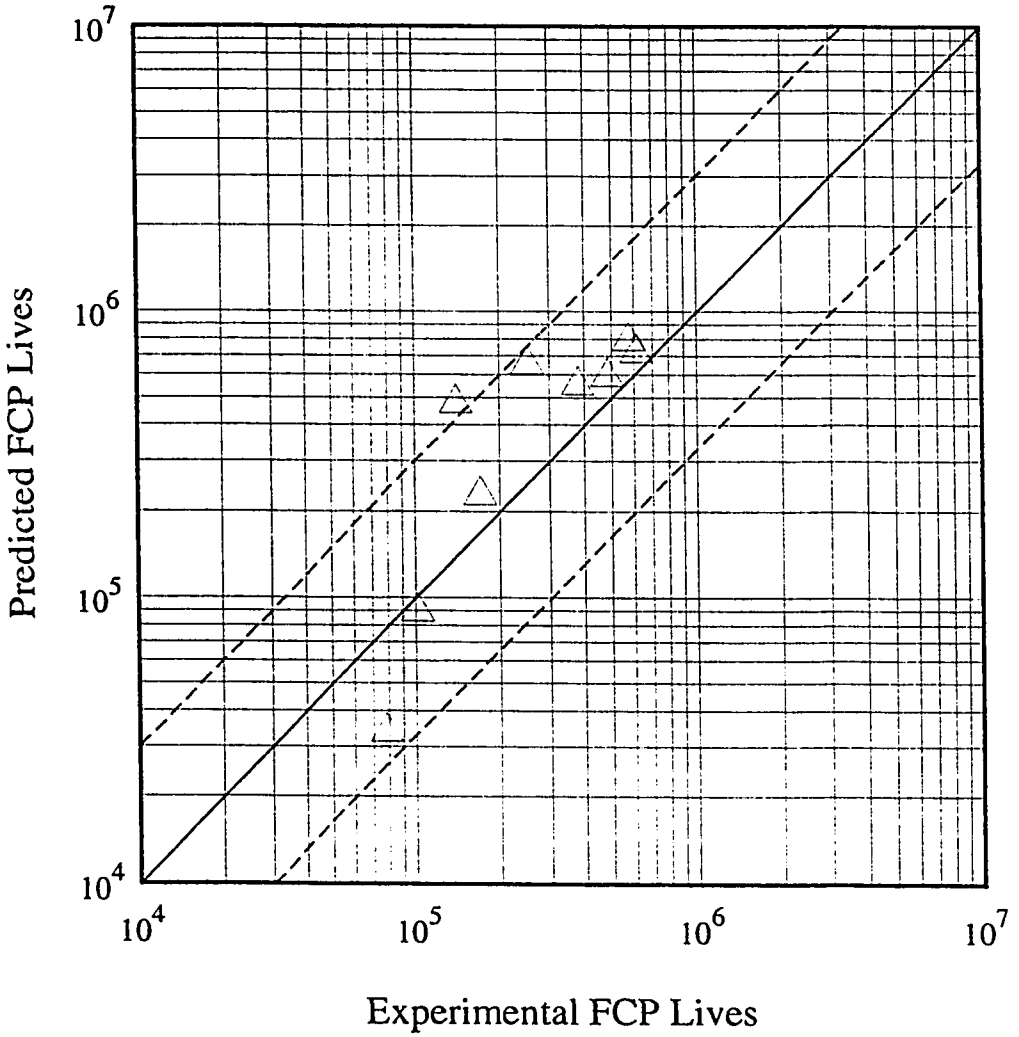

Figure 5.13: Fatigue Lives; Experimental Vs Wheeler's prediction (using Modified Paris equation).

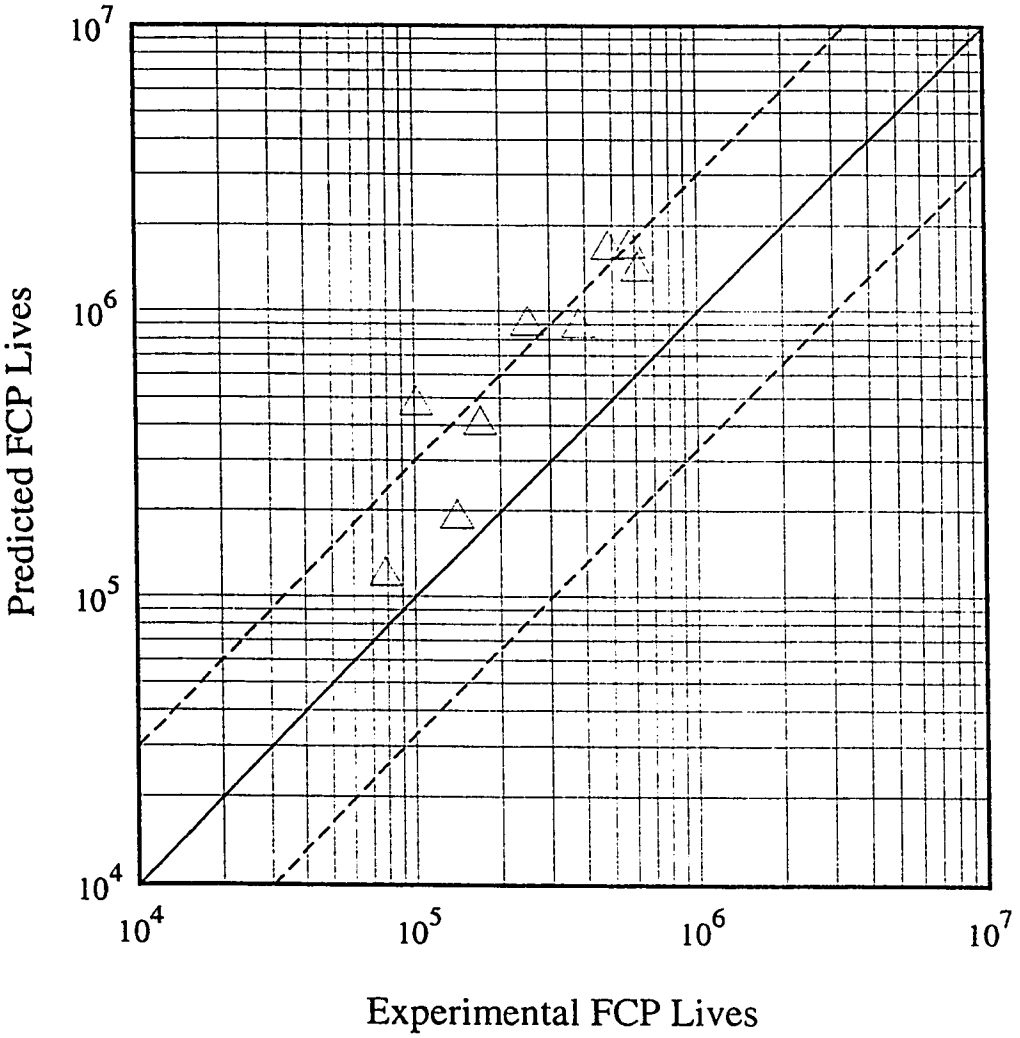

Figure 5.14: Fatigue Lives; Experiment Vs Elber's model prediction.

Chapter 6

Analysis Of The Results

6.1 Effect of Magnitude of OL on FCG Rate

Under similar conditions when the magnitude of OL is increased from 9KN (OL ratio 1.5) to 13KN (OL ratio 2.17), the fatigue life is decreased as seen from Fig. (6.1). At 13KN the a Vs N curve almost becomes identical to the CAL curve. This means that the retardation effect due to overload diminishes at OL ratio 2.17. A similar observation was also reported by Ohrloff [50].

While analysing the FCG rate curve it was observed that the FCG rate increases with the increase in the OL magnitude. However, the crack growth retardation is still observed at all OL ratios when compared with constant amplitude loading Fig. (6.2). Jones [53] has also reported that the OL ratio could be used as an indication

of the amount of subsequent retardation.

6.2 Effect of Number of Cycles on FCG Rate

It is interesting to note that with the decrease in the base number of cycles (n) of CAL from 5000 to 1000, the fatigue life is decreased considerably, but further decrease in the number of base cycles to 100 show an increase in fatigue life compared to n=1000 cycles. This trend is more close to the n=5000 cycles Fig. (6.3). The reason for this behavior is not clearly understood and need further investigation.

6.3 Effect of Multiple OLs on FCG Rate

Number of OL peaks when increased from one to five, each with the same magnitude, produce an acceleration in crack growth rate when compared to the single OL under same conditions Fig.(6.6). But corresponding to the CAL there is a definite retardation.

Residual compressive stersses that is produced by the surrounding elastic material is decreased as the number of overloads increase. This caused the crack to travel lesser distance in the plastic zone, hence is not as much retarded as under single OL. Crack closure effects are also reduced with multiple OL's application as compared to single OL.

6.4 Fatigue Crack Propagation Lives

6.4.1 Wheeler's Model (using Paris equation)

The predicted FCP lives calculated from the Wheeler's model using the Paris equation show a good agreement with the experimental findings within a factor of three which is a reasonably good prediction for fatigue under variable amplitude loading. For n=5000 the result is the most non-conservative.

6.4.2 Wheeler's Model (using modified Paris equation)

The predicted FCP lives calculated from the Wheeler's model using the modified version of Paris equation show even a better agreement with the experimental results. This improvement in the fatigue life estimation occurs due to the use of the stress ratio in the form of $\frac{1+R}{1-R}$ in the formulation.

6.4.3 Elber's Model

The predicted FCP lives calculated from the Elber's model using the effective ΔK concept is more non-conservative in predicting the FCP lives when compared with the Wheeler's models (as discussed earlier). All the data points are seen lying above the perfect correlation line (solid line). This deviation may be attributed to the inability of this model to take to account the OL ratio effect which we have seen to effect the FCP rates.

6.5 FCG Rate From Fractography

Comparing the fractographic data with the experimental data generated by Instron 8501 we observe that the FCG rate is consistent in the two approaches (see Figs. 6.7 to 6.10). Nevertheless, the general trend of the fractographic data show good agreement with the experimental results.

Following comments can be made from the results of fractographic study:

- Striations were ill defined in general.
- Clear sites were not easily detected.
- Striations were only resolved at one end of the fractured surface.
- Striations were best resolved when OL's were less spaced.
- High magnitudes of OL's resulted in tearing of the metal which restricted the chances of resolving the striations.

The above factors can be attributed to the relativly small thickness of the samples.

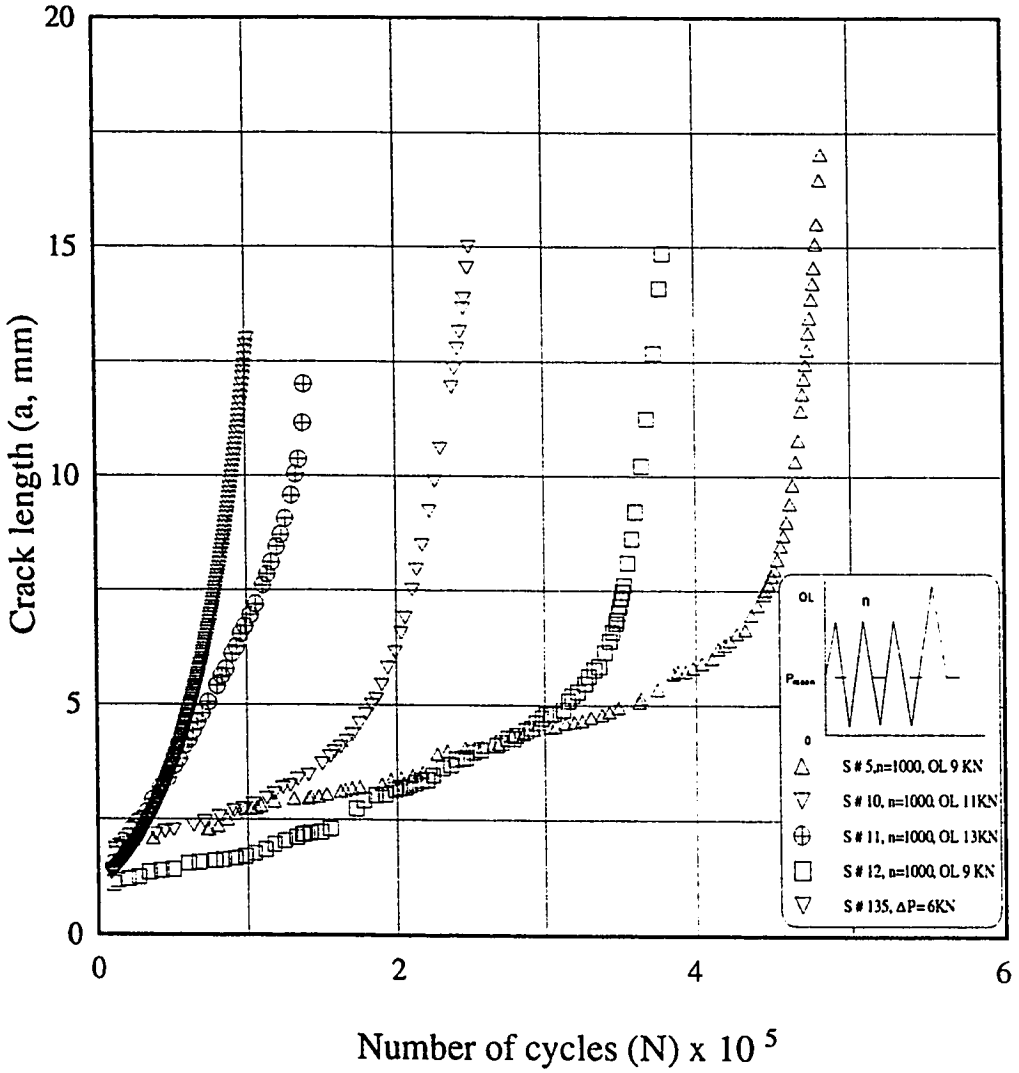

Figure 6.1: a vs N curve showing the OL magnitude effect.

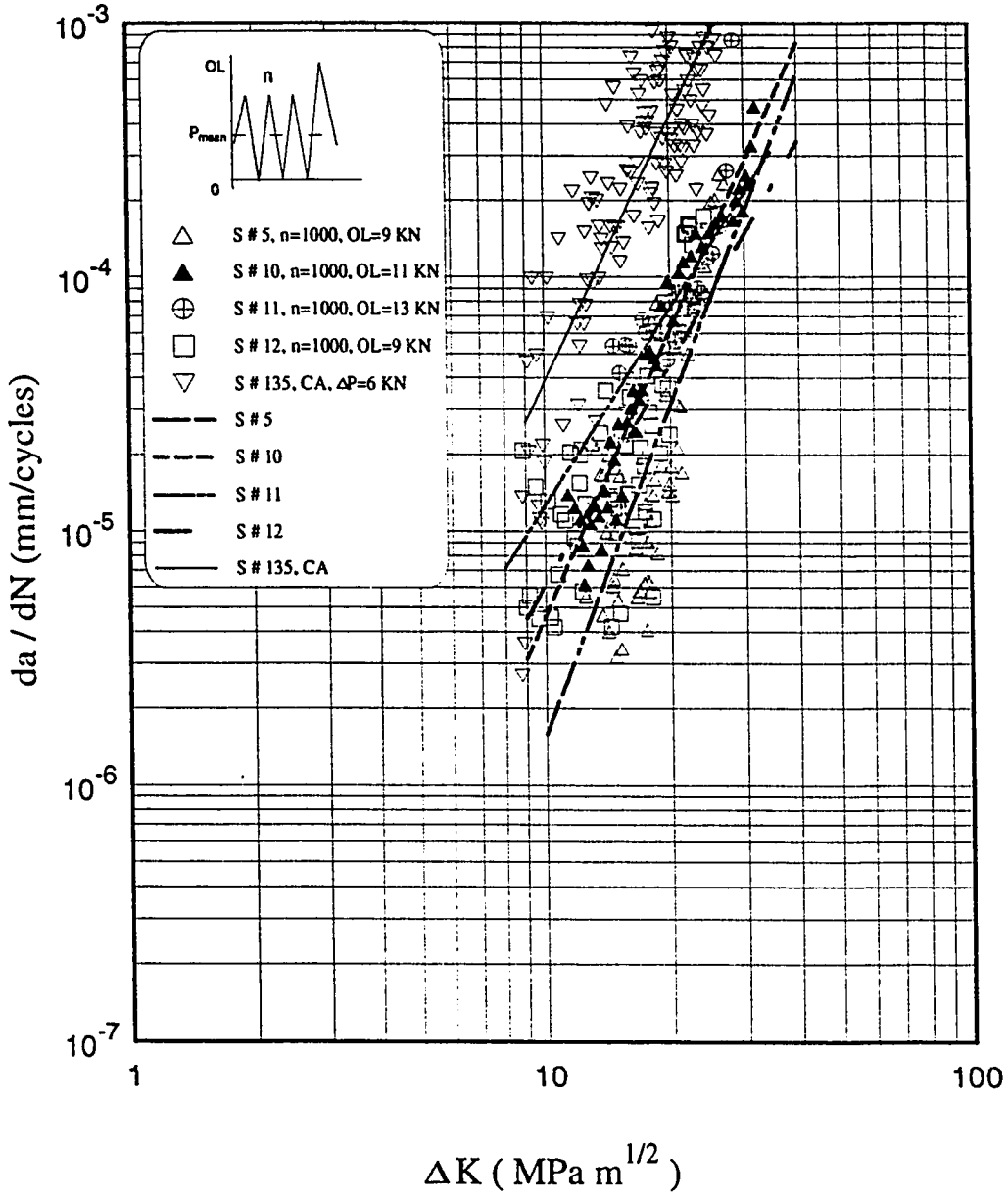

Figure 6.2: FCG rate vs ΔK showing OL magnitude effect.

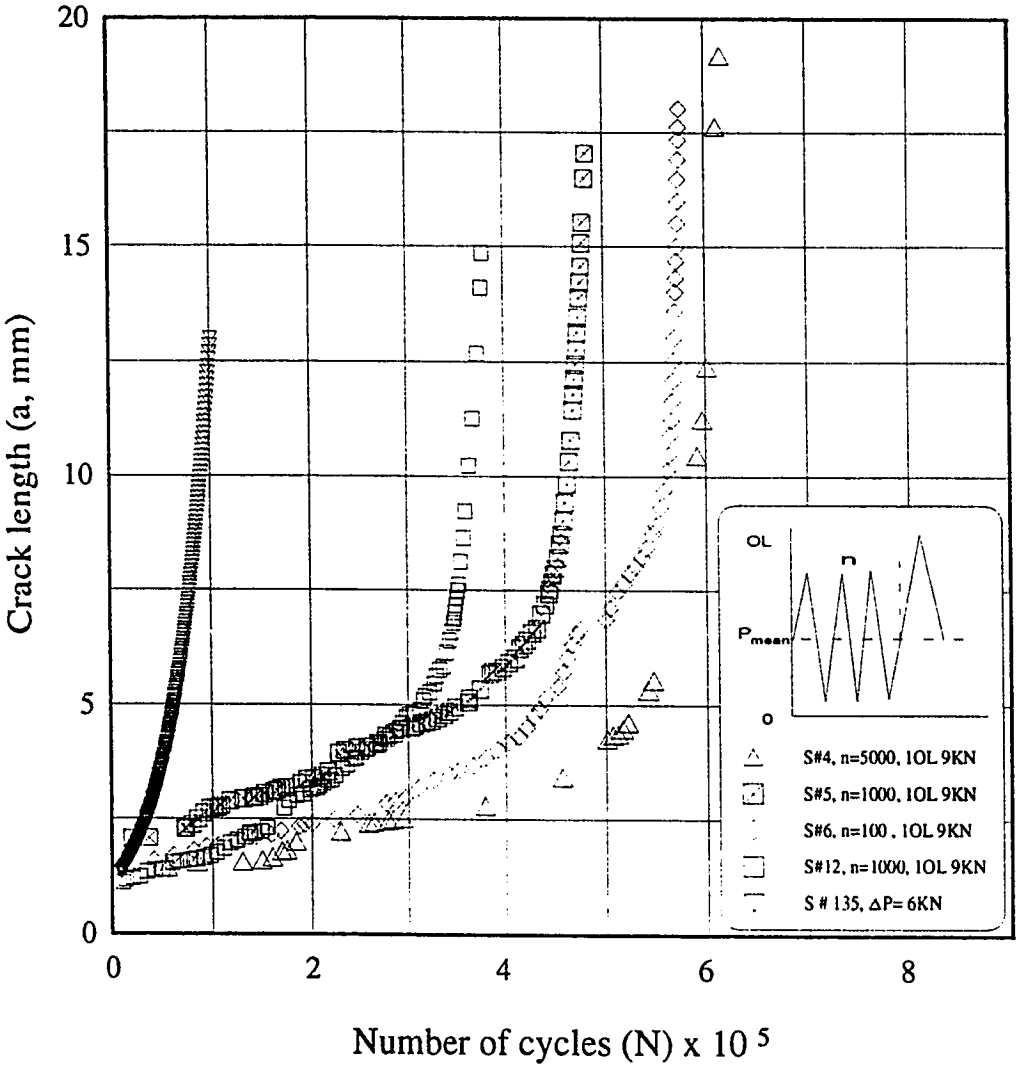

Figure 6.3: *a* vs *N* curve showing the effect of number of base CAL cycles.

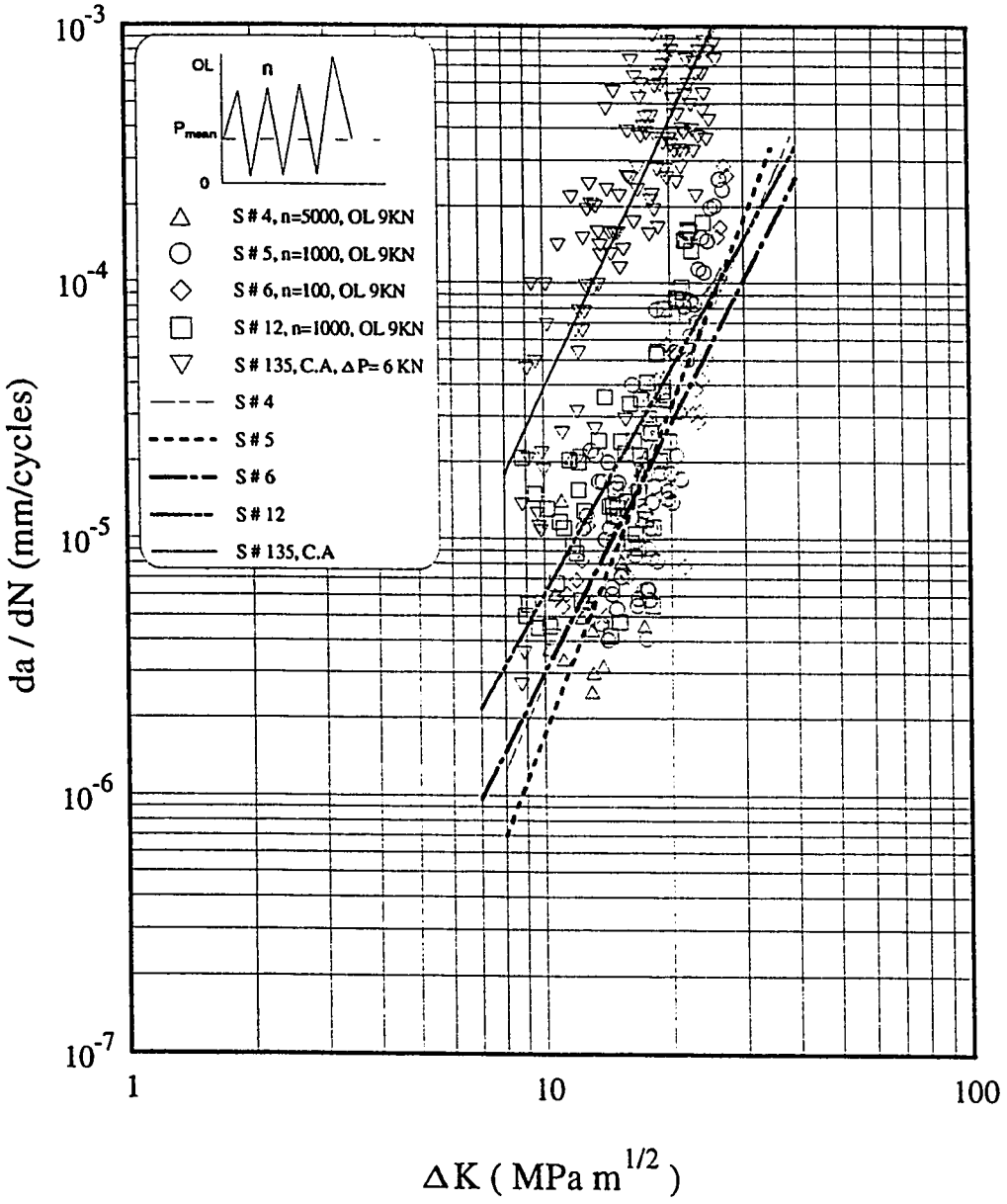

Figure 6.4: FCG rate vs ΔK showing the effect of number of base cycles.

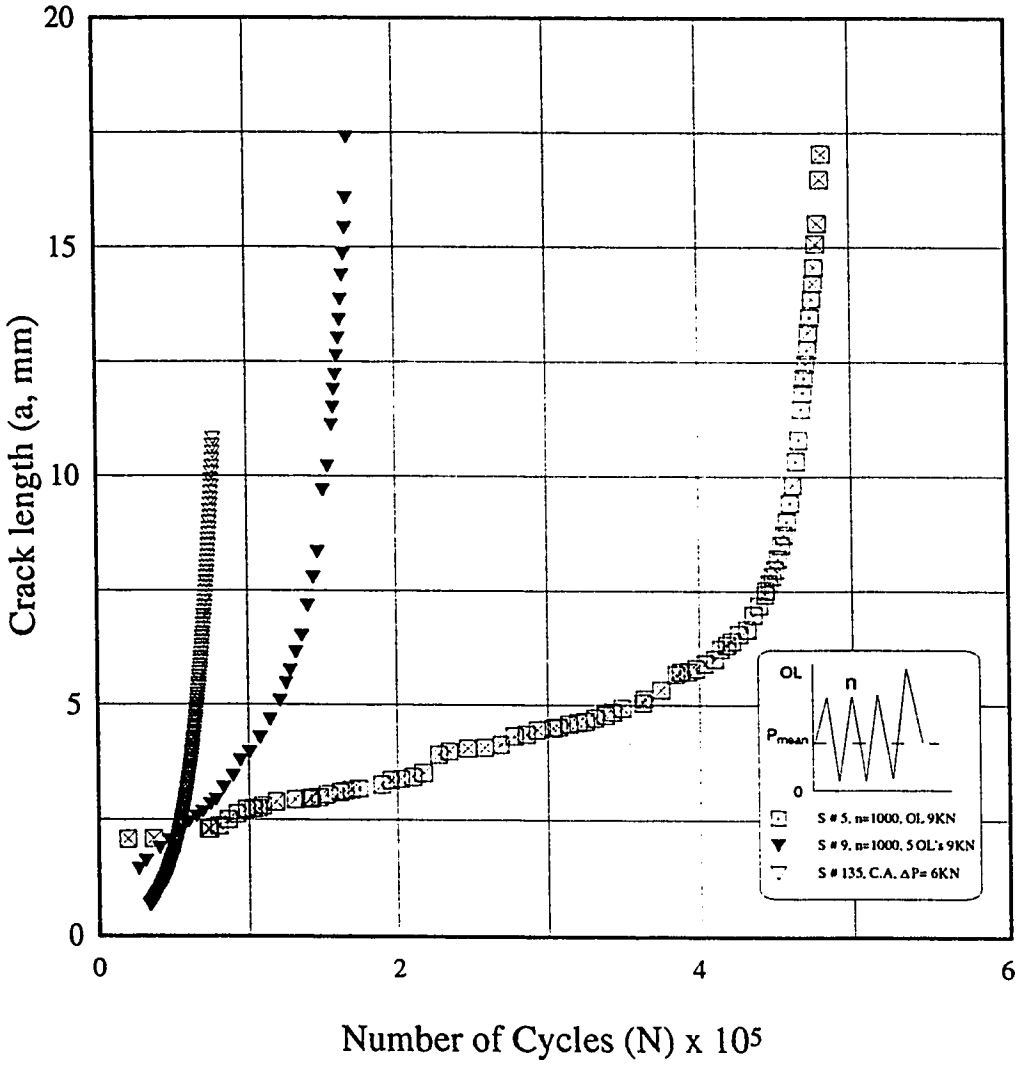

Figure 6.5: a vs N curve showing the effect of multiple OLs.

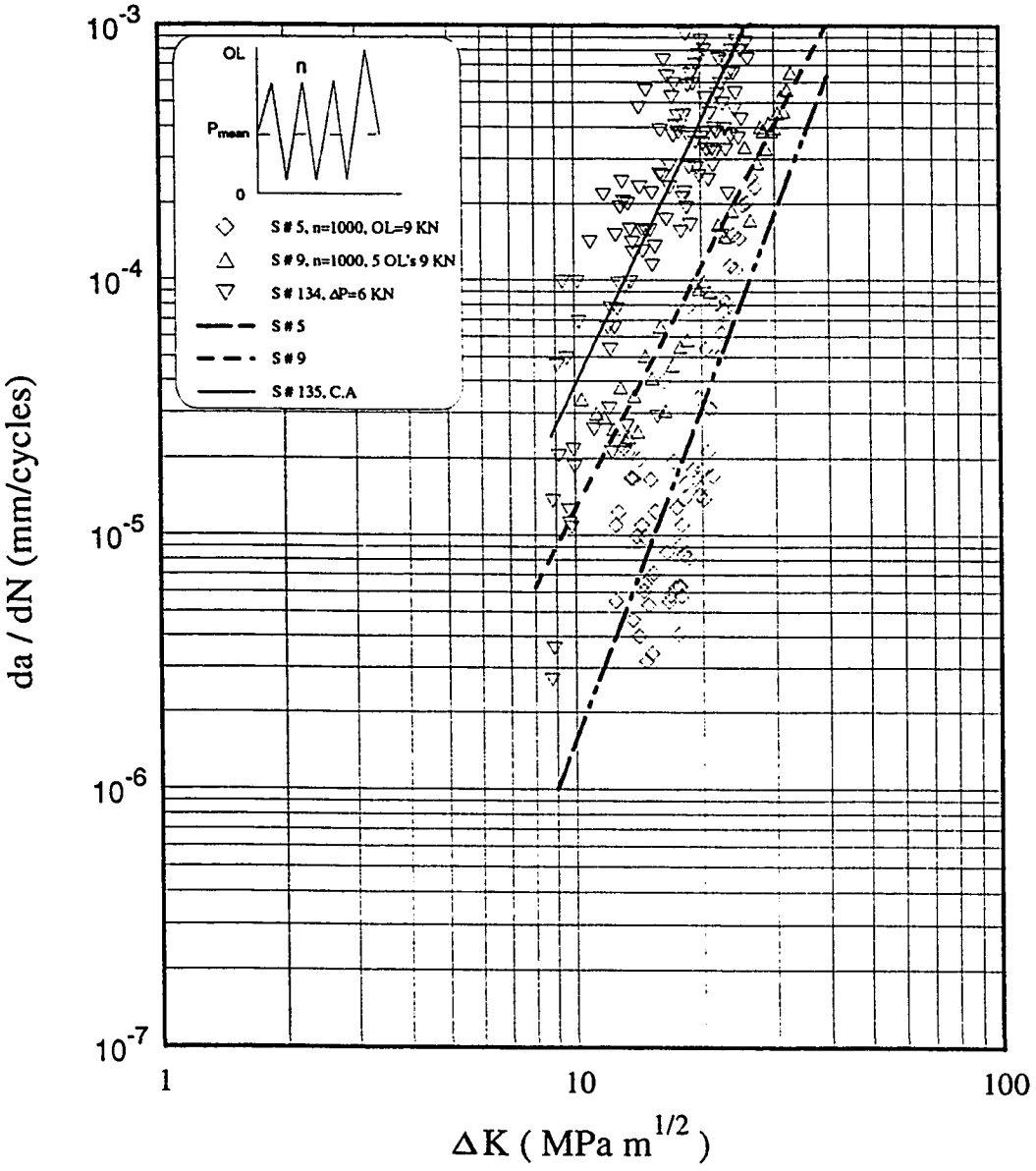

Figure 6.6: FCG rate vs ΔK showing the effect of multiple OLs.

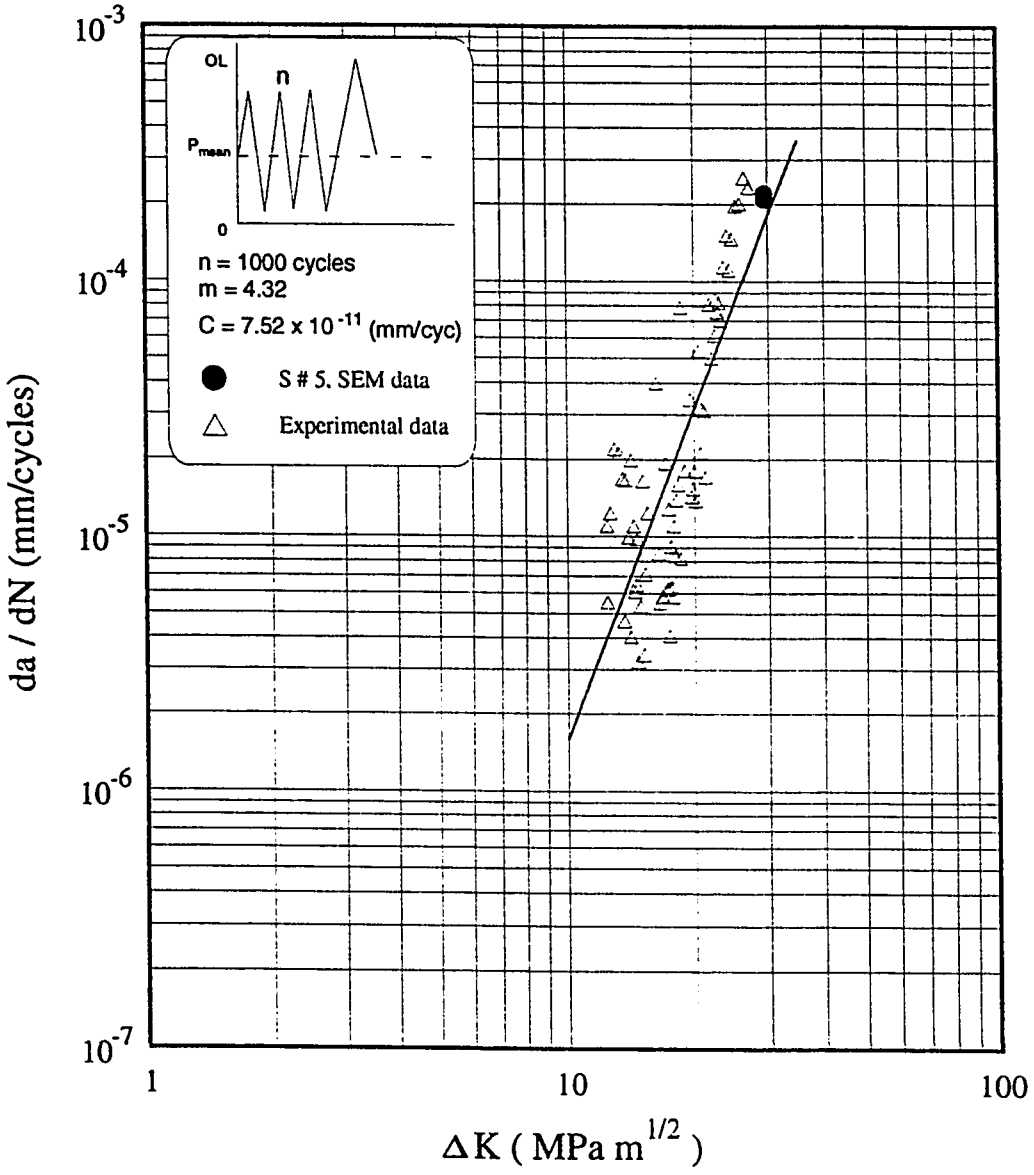

Figure 6.7: Comparison of FCG rate Vs ΔK (for S # 5, n=1000, 10 Hz and single OL at 9KN), with experimental and fractographic data.

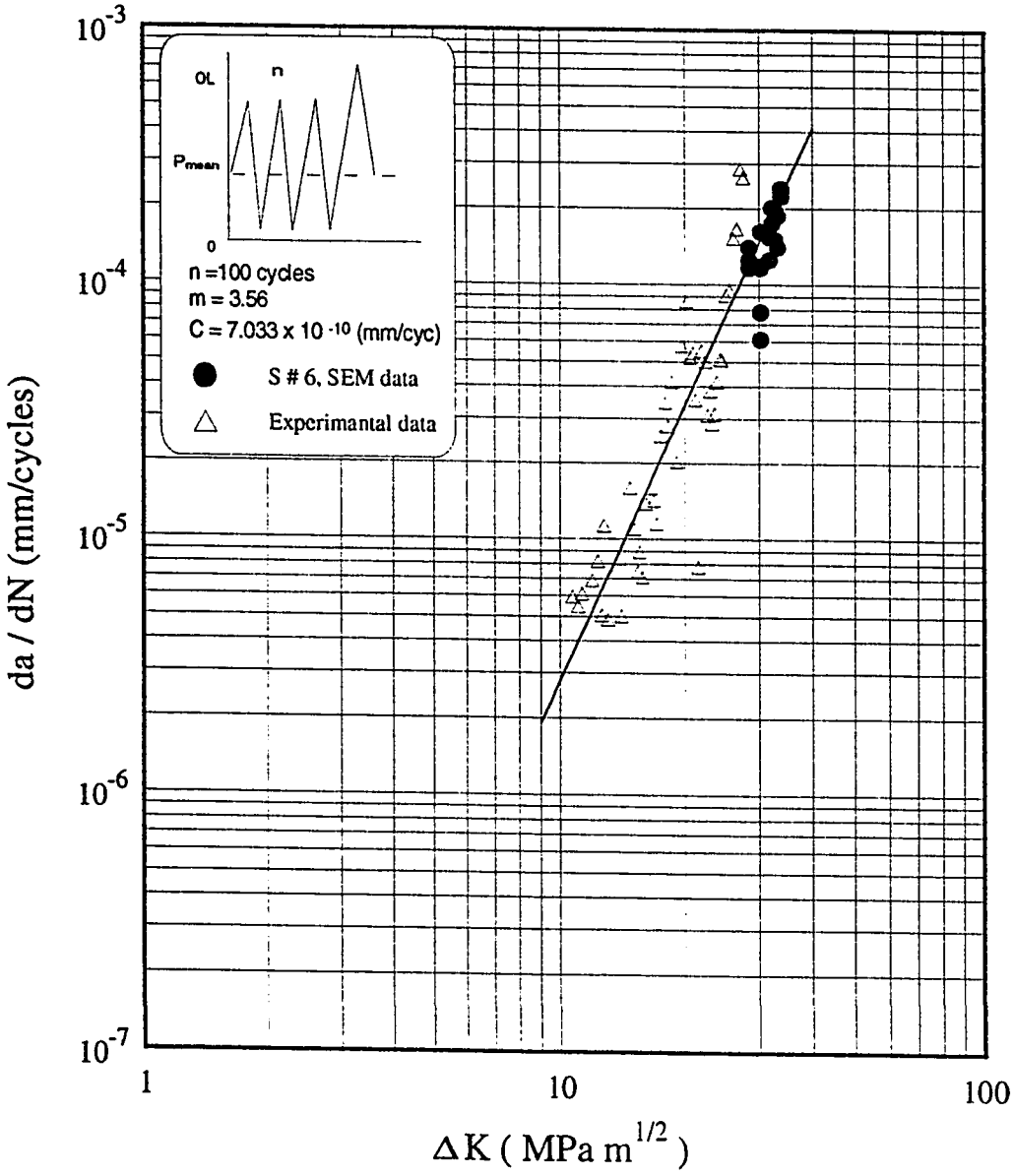

Figure 6.8: Comparison of FCG rate Vs ΔK (for S # 6 , n=100, 10 Hz and single OL at 9KN), with experimental and fractographic data.

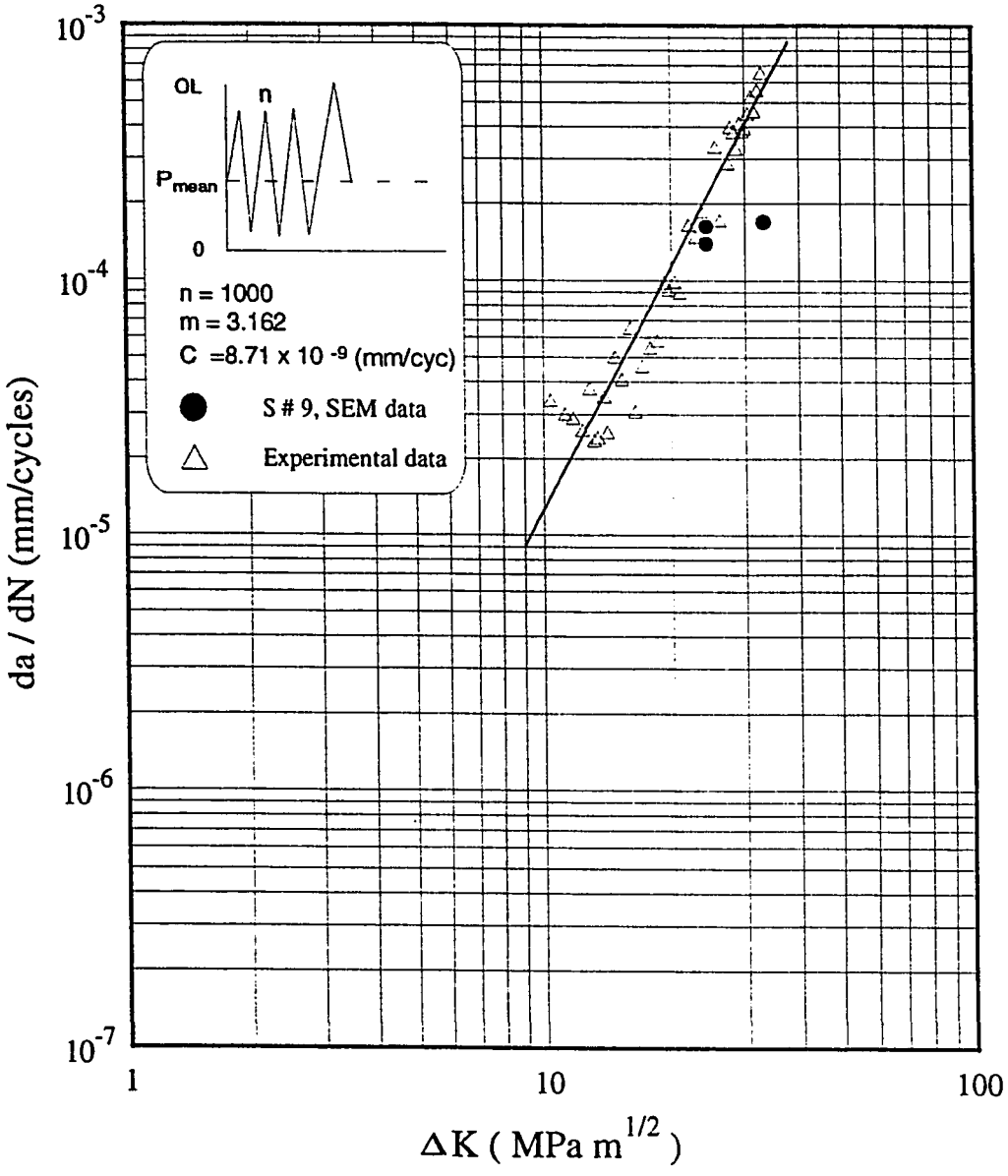

Figure 6.9: Comparison of FCG rate Vs ΔK (for S # 9, n=1000, 10 Hz and five OLs at 9KN), with experimental and fractographic data.

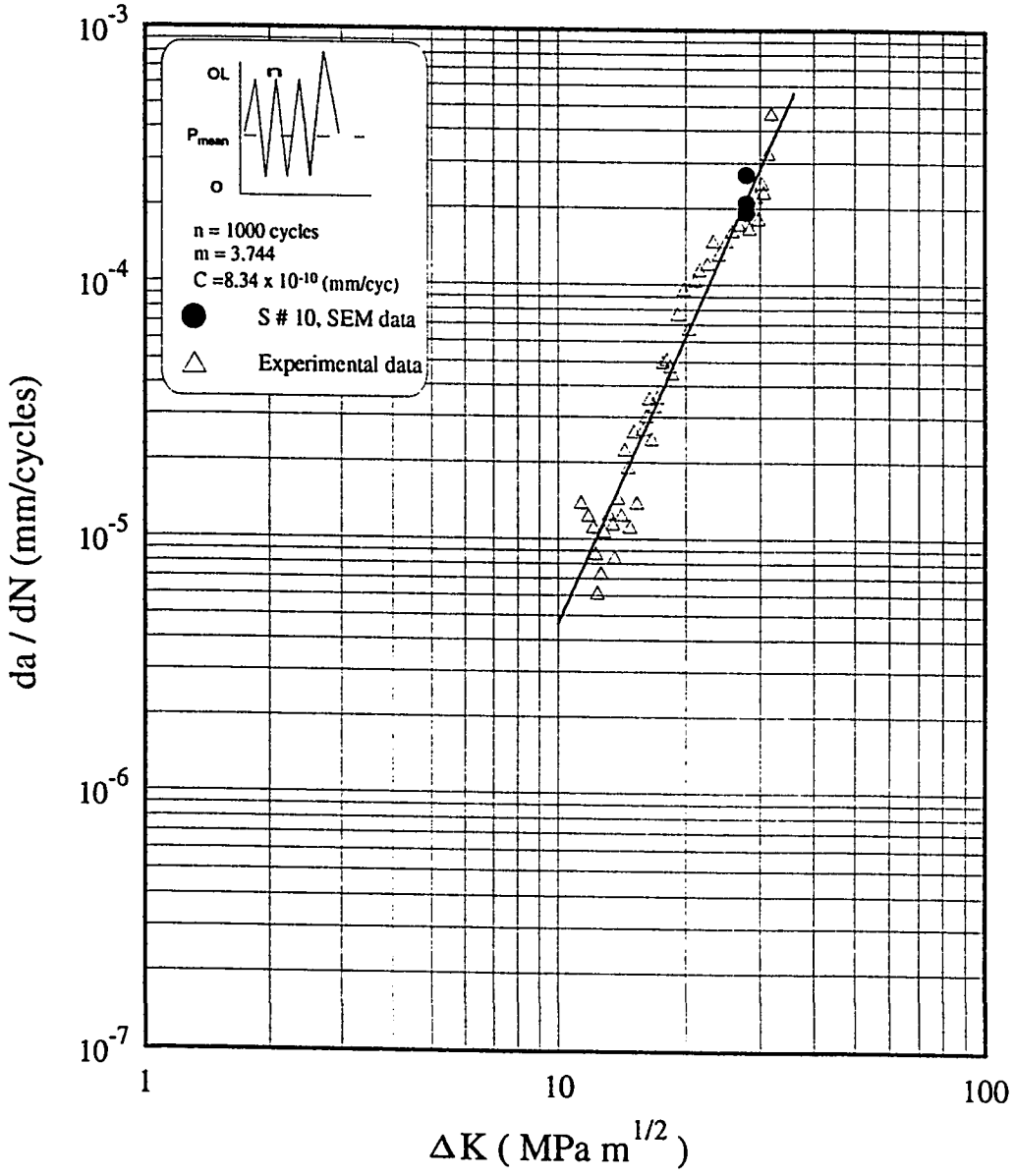

Figure 6.10: Comparison of FCG rate Vs ΔK (for S # 10, n=1000, 10 Hz and single OL at 11KN), with experimental and fractographic data.

Chapter 7

Conclusion and Suggestions

7.1 Conclusion

7.1.1 Load Interaction Effect

It is clear from the results obtained here that load interation effect under the influence of OLs, produces definite retardation in the fatigue crack growth rate and consequently, the fatigue crack propagation life is increased.

Keeping the number of CAL cycles (base cycles) same, when the magnitude of OL is increased from 9KN (OL ratio 1.5) to 13KN (OL ratio 2.17), the fatigue life is decreased. With the decrease in the *base number of cycles* (n) of CAL from 5000 to 1000, the fatigue life is decreased considerably, but further decrease in base cycle

number to 100 show an increase in fatigue life compared to n=1000 cycles and approaches that of n=5000 cycles.

When the number of OL peaks are increased from one to five (each with the same magnitude), an acceleration in crack growth rate occurs when compared to the single OL peak. But compared to CAL a definite retardation is observed inall cases.

7.1.2 FCP Lives

Reasonably good predictions of fatigue crack propagation lives under variable amplitude loading can be obtained using all the three modified constant amplitude loading models discussed. The results show that the Wheeler's model using Paris equation gives reasonable fatigue crack propagation life predictions under variable amplitude loading conditions. While the Wheeler's model using modified Paris equation improves fatigue crack propagation life predictions. Elber's crack closure model on the other hand slightly over predicts fatigue crack propagation lives for all cases.

In the order of preference for analytical fatigue life prediction models under variable amplitude loading, the three models discussed may be ranked as Modified Paris model, the Paris model and the Elber's model.

7.1.3 Fractographic Results

Fractographic study by analysing the fatigue striations was used to correlate the observed experimental macroscopic crack growth rates with the microscopic growth rates by using electron microscope. The results show a very good agreement with the two methods of analysis. This strengthens our confidence in the experimental data and hence the analytical fatigue life predictons.

The results from the fractograph can be used to predict the fatigue propagation life. This is possible when these results are used to calculate the paris constants C and m. Once these constants are obtained for each specimen, same analytical approach (as described in chapter three) can be applied to obtain the fatigue life predictions using the fractographic approach.

7.2 Suggestions For Future Work

Like most research endavours, it is not possible to cover the various aspects of the multidimentional nature of the problem in hand. There is a lot of room for future research in this reletively new field. Some areas are mentioned below.

- More complex block variable amplitude loading loading could be investigated.
- Effect of frequency and stress ratio may be studied.
- Effect of thickness on fatigue crack growth rates could be explored.
- Effect of environment under variable amplitude loading may be explored.
- Effect of surface finish may be investigated.
- This work could be extended to include newly developed high strength materials, polymers and composites.
- Instead of simple block variable amplitude loading, all of the above may be investigated under random loading to give more realistic predictions.

Bibliography

[1] J. J. Coner Julie A. Bannantine and J. Hand Rock. Fundamentals of metal fatigue analysis. *Printice Hall*, 1990.

[2] H. Misawa A. Fukushima, Y. Kawakami. Effect of very small number of stress cycles above fatigue limit on FCP under VAL. *Bulletin of JSME*, V-28, n-238-3:578–585, 1985.

[3] C. M. Ward-Close and A. F. Blom. Mechanisms associated with transient FCG under VAL : an experimental and numerical study. *Engineering Fracture Mechanics*, V-32, n-4:613–638, 1989.

[4] D. V. Nelson. Effect of residual stress on FCP. *Residual Stress effects In Fatigue, ASTM STP 776, Ed. J. F. Throp*, pages 172–194, 1982.

[5] L. P. Pook N. E. Frost and K. Marsh. Metal Fatigue. *Oxford University Press*, 1974.

[6] O. Vardar. Effect of single OL in FCP. *Engineering Fracture Mechanics*, V-30, n-3:329–335, 1988.

[7] Fatigue reliability : Introduction. *ASCE Journal of Structural Division*, V-108, n-1:3–89, 1982.

[8] J. F. Knott and A. C. Picard. Effect of OL in FCP : Alluminum Alloys. *Metallurgical Science*, pages 399–421, Aug/Sept 1977.

[9] W. J Mills and R. W. Hertzberg. Load interaction effect on FCP in 2024-T3 aluminum alloy. *Engineering Fracture Mechanics*, V-8:657–667, 1976.

[10] R. P. Wei and T. T. Shih. Delay in FCG. *International Journal of Fatigue*, V-10:77–85, 1974.

[11] P. J. Bernard and C. E. Richards. Methods for comparing fatigue lives for spectrum loading. *Metarial Science*, pages 390–398, 1977.

[12] K. T. Venkateswara Rao and R. O. Ritchie. Fatigue of aluminum-lithium alloys. *International Materials Review*, V-37.n-4:153–185, 1992.

[13] P. Paris and F. Erdogan. A critical analysis of crack propagation laws. *Journal of Basic Engineering*, pages 528–534, Dec. 1963.

[14] D.W.Hoeppner and W.E.Krupp. Prediction of component life by application of FCG knowledge. *Engineering Fracture Mechanics*, V-6:47–70, 1974.

[15] H. J. C. Voorwald and C. C. E. Pinto Jr. Modelling of FCG following OLs. *International Journal of Fatigue*, V-13, n-5:423–427, 1991.

[16] M. A. Bieniek T. V. Kutt. Cumulative damage in fatigue life prediction. *AIAA, Juornal*, V-26, n-2:213–219, 1988.

[17] Aurthur J. McEvily and Kunori Minakawa. Crack closure and variable amplitude FCG. *Basic Questions in Fatigue ASTM. STP 924*, V-1:357–375, 1988.

[18] R. G. Forman and V. E. Kearney. Numerical analysis of crack propagation in cyclic loaded structures. *Transactions of ASME, Journal of Basic Engineering*, V-D89, n-3:459–464, 1967.

[19] Karl-Heinz Schwalbe. Comparison of several FCP laws with experimental results. *Engineering Fracture Mechanics*, V-6.:325–314, 1974.

[20] P. and W. Schutz. Assessment of concepts of FCI and FCP life predictions. *Z. Werkstofftech*, V-17:397–456, 1986.

[21] W. Geary. A review of some aspects of FCG under VAL. *International Journal of Fatigue*, V-14, n-6:377–386, 1992.

[22] D. E. Sochie and C.T. Hua. Fatigue damage in 1045 steel under VAL biaxial loading. *Fatigue and Fracture of Engineering Materials and Structure*, V-8 ,n-2:101–114, 1985.

[23] H. Alawi. Designing reliability for FCG under VAL. *Engineering Fracture Mechanics*, V-37,n-1:75–85, 1990.

[24] S. Matsuoka H. Masuda. Mechanism of corrosion FCP in steels under VAL. *Corrosion Science*, V-30, n-6/7:631–642, 1990.

[25] J. Schijve S. Zhang, R. Marrissen and K. Schulte. Crack propagation studies on Al 7475 on the basis of constant amplitude and selective VAL histories. *Fatigue and Fracture of Engineering Materials and Structure*, V-10:315–332, 1987.

[26] R. C. Rice et. al. Consolidation of fatigue and FCP data for design use, prepared by Beattell Columbus Laboratories, Columbus, Ohio, NASA CR-2586. Oct. 1975.

[27] C. Hahn and R. Simon. A review of FCG in high strength aluminum alloys and relevant metallurgical factors. *Engineering Fracture Mechanics*, pages 523–540, 1973.

[28] T. Akyurek and O. G. Bilir. A survey of FCG life estimation methodologies. *Engineering Fracture Mechanics*, V-42, n-5:797–803, 1992.

[29] X. P. Zhang P. Johnson and G. Pluvinage. Crack growth rate in impact fatigue under programmed VAL fatigue. *Engineering Fracture Mechanics*, V-37,n-3:519–525, 1990.

[30] T. R. Porter. Method of analysis and prediction for variable amplitude FCG. *Engineering Fracture Mechanics*, V-4:717–736, 1972.

[31] J. Solin. Methods for comparing fatigue lives for spectrum loading. *International Journal of Fatigue*, V-12, n-1:35–42, 1990.

[32] F. C. Hamel et. al. A simple procedure for the prediction of the FCGR under VAL. *Fatigue life : Analysis and prediction, Ed. V. S. Geol, ASM*, pages 275–281, 1985.

[33] J. Polak A. Vasek. Low cycle fatigue damage accumulation in Aromco-Iron. *Fatigue and Fracture of Engineering Materials and Structure*, V-14, n-2/3:193–204, 1991.

[34] C. M. Sonsino. Limitations in the use of RMS values and equavilent stress in VAL. *International Journal of Fatigue*, V-11, n-3:142–152, 1989.

[35] M. Gabra and C. Bathias. Interpretation of FCG in aluminum alloys under programmed block loading. *Fatigue and Fracture of Engineering Materials and Structure*, V-7, n-4:285–298, 1984.

[36] A. J. McEvily. On quantative analysis of FCP. *Fatigue Mechanisms: Advances in quantative measurement of Physical Damage, ASTM STP 811, Ed. Lankford et. al.*, pages 283–312, 1983.

[37] A. Sugeta and M. Jano. Estimation method of elastic plastic FCGR under VAL. *Key Engineering Materials*, V-51 and V-57:277–282, 1985.

[38] D. L. Davidson and J. Lankford. FCG in metals and alloys, mechanisms and micromechanisms. *International Materials Review*, V-32, n-2:45–76, 1992.

[39] J.Schijve. Predictions on fatigue. *JSME, International Journal, Series I*, V-34, n-3:269–280, 1991.

[40] J. M. Barsom. FCG under VAL in ASTM A 514 grade B steel. *ASTM STP No 536*, 1987.

[41] T. H. Topper D. DuQuesnay and R. Jurcevic. A new fatigue life prediction model for VAL. *Fatigue and Fracture Mechanics, Localized Damage.Ed. H. Nishitani, Elsevier Applied Sc.*, V-1:105–120, 1992.

[42] R. Pippan and J. Golos. A comparasion of different methods to determine the threshold of FCP. *International Journal of Fatigue*, V-16, n-8:579–582, Nov-1994.

[43] F. P. Packman. On the influence of single and multiple OL on FCP in 7075-T6511 aluminum. *Engineering Fracture Mechanics*, V-5:479–497, 1973.

[44] S. Matsuoka and K. Tanaka. The retardation phenomenon of FCG in HT 80 steel. *Engineering Fracture Mechanics*, V-8:507–523, 1976.

[45] A. T. Alpas and C. N. Reid. The effect of R ratio on near threshold FCG in a metallic glass and stainless steel. *Engineering Fracture Machanics*, V-36, n-1:72–92, 1990.

[46] G. Henaff and J. Petit. FCP behavior under VAL in near threshold region of a high strength alloy steel. *Fatigue and Fracture of Engineering Materials and Structure*, V-15 ,n-1:1155–1170, 1972.

[47] K. L. Carlson and G. A. Kardomateas. Effects of compressive load excursions on FCG. *International Journal of Fatigue*, V-16, n-2:141–146, Feb. 1994.

[48] T. Shih and R. P. Wei. A study of crack closure in fatigue. *Engineering Fracture Mechanics*, V-6:19–32, 1974.

[49] J. M. Barsom. FCP in steels of various yield strengths. *Transactions of ASME, Journal of Engineering for Industry*, Series B. n- 4, Nov. 1971.

[50] A. Gysler N. Ohrloff and G. Lutjering. FCP behavior under VAL. *FCP under VAL, Ed. J. Petit, D. Davidson and P. Rabbe. Elsevier Science Publication*, pages 24–34, 1988.

[51] T. Nosho et. al R. Koterazawa. Acceleration of FCG under intermittent over-stressing with different mean stress levels. *Fatigue and fracture in engineering materials and structures*, V-17, n-9:1033–1041. 1994.

[52] Keiji Ogura and K. Ohji. FEM analysis of crack closure and delay effects inFCP under VAL. *Engineering Fracture Mechanics*, V-9:471–480, 1977.

[53] R. E. F. Jones. FCGretardation after single cycle peak OL in Ti-6Al-4V, titanium alloy. *Engineering Fracture Mechanics*, V-5:585–604, 1973.

[54] S. G. Russel. A new model for FCG retardation following an OL. *Engineering Fracture Machanics*, V-33, n-6:839–854, 1989.

[55] S. Zhang et. al. Systematic fracture surface analysis for the evaluation of crack closure concept. *FCG under VAL, Ed. J. Petit, D. Davidson and P. Rabbe Elsevier Science Publication*, pages 48–63, 1988.

[56] R. J. Allen. A review of fcg characteristics by lefm, part iii. *Fatigue and Fracture of Engineering Materials and Structure*, V-11,n-2:45–108, 1988.

[57] C. Bathias and M. Vancon. Mechanisms of OL effect in FCP in aluminum alloys. *Engineering Fracture Mechanics*, V-10:409–424, 1978.

[58] W. M. Thomas. The effect of single OL upon fatigue crack in 5083-H321 aluminum. *Engineering Fracture Mechanics*, V-23:1015–1029, 1986.

[59] A. S. L. Chang X. Zhang and G. A. O. Davis. Numerical simulation of FCG under computer complex loading sequences. *Engineering Fracture Mechanics*, V-42, n2:213–216, 1992.

[60] R. O. Ritchie and W. Yu. FCP in 2090 Al-Li alloy: effect of compressive OL cycles. *Journal of Engineering Matallurgical Technology*, n-109:81–85, 1987.

[61] R. O. Ritchie. *Engineering Fracture Mechanics*, V-22:35, 1985.

[62] T. H. Topper and M. T. Yu. The effect of material strength, stress ratio and compressive OL on the threshold behavior of SAE 1045 steel. *Journal of Engineering Matallurgical Technology*, V-107:19–25, 1985.

[63] Ryoichi Koterazawa. Acceleration of fatigue and creep crack propagation under VAL. *Fatigue Life: Analysis and Prediction, Ed. V. S. Goel, ASM*, pages 187–196, 1985.

[64] W. Elber. Fatigue crack closure under cyclic tension. *Engineering Fracture Machanics*, V-2:37–45, 1970.

[65] W. Elber. The significant of crack closure. *ASTM STP No 486. Ph.*, pages 230–242, 1971.

[66] D. Broek. A critical note on electron fractography. *Engineering Fracture Mechanics*, V-1:691–695, 1970.

[67] M. N. Georgier and N. Ya Mezhova. Determination of FCPR by the electron fractograph method. *Soviet Materials Science (Translated from Russian*, V-21, n-21:161–163, March-April 1985.

[68] M. R. Ling. Fractographic analysis of crack growth from shear lip development under simple VAL. *Fatigue and Fracture of Engineering Materials and Structure*, V-13,n-5:443–456, 1990.

[69] A. Fatemi R. I. Stephens and C. M. Wang. Variable amplitude fatigue crack initiation and growth on five carbon or low alloy cast steels at room temperature. *Fatigue at Low Temperature, Ed. R. I. Stephens, ASTM STP 857*, pages 293–312, 1985.

[70] Takeo Yokobori and K. Sato. The effect of frequency on FCPR and striation spacing in 2024-T3 aluminum alloy and SM-50 steel. *Engineering Fracture Mechanics*, V-8:81–88, 1976.

[71] John M. Barsom and Stanley T. Rolfe. Fracture and fatigue control in structures: Application of Fracture Mechanics. *second edition. Printice Hall*, 1987.

[72] O. Wheeler. Spectrum loading and crack growth. *Journal of ASME Transactions*, pages 181–186, March 1972.

[73] L.P. Pook. *Developments in fracture mechanics*, volume V-1. Applied Science Publishers Ltd, London. 1983.

[74] S. Kocanda. Fatigue and fracture of metals, Published by, Sijthoff and Noordhoff Int'l. 1978.

[75] W. H. Schlosberg and J. B. Cohen. The plastic zone and residual stress near a notch and a fatigue crack in HSLA steel. *Metallurgical Transactions A*, V-13-A:1987–1995, 1982.

[76] J. T. Sparrow J. W. Hearl and P. M. Crose. The use of SEM. *Pragmon Press Ltd.*, 1972.

[77] L.P. Pook. *Developments in fracture mechanics*, volume V-11. Applied Science Publishers Ltd, London, 1983.

[78] A. Buch. Verification of FCI life prediction results. *Technical Institute of Technology, Haifa, TAE, No 400*, 1980.

[79] Ali Fatemi and D. F. Socie. A critical plane approach to multiaxial fatigue damage inducing out of phase loadings. *Fatigue and fracture of Engineering Materials and Structures*, V-11, n-3:149–169. 1988.